BULLETIN DE L'INSTITUT ROYAL DES SCIENCES NATURELLES DE BELGIQUE
BULLETIN VAN HET KONINKLIJK BELGISCH INSTITUUT VOOR NATUURWETENSCHAPPEN

SCIENCES DE LA TERRE, 70: 25-52, 2000
AARDWETENSCHAPPEN, 70: 25-52, 2000

Graphic correlation of Frasnian sections (Upper Devonian) in the Ardennes, Belgium

by Sofie GOUWY & Pierre BULTYNCK

Abstract

A high-resolution correlation of 10 Frasnian sections in the Belgian Ardennes is made using the graphic correlation method. The measured ranges of 85 conodont taxa, 48 coral taxa, 29 brachiopod taxa and one stromatoporoid taxon have been assembled into a chronostratigraphic framework. The Ardennes Frasnian Regional Composite developed in this study provides a higher stratigraphic resolution than the traditionally used conodont zonation. It allows a subdivision of the Frasnian into 532 composite standard units derived from the standard reference section in the southern part of the Dinant Synclinorium, completed with a section in the Philippeville Massif for the uppermost part of the Frasnian that is not exposed in the southern part of the Dinant Synclinorium, units 332-532. By correlating the sections using time-equivalent lines, the diachronous pattern of the deposits becomes clearly visible. The combination of this pattern and the conodont biofacies changes in the sections were used to recognise four major third order (500.000y-5m.y.) transgression-regression cycles. The first one, starting in the latest Givetian (Early *falsiovalis* Zone), continues through the *transitans* Zone and ends in the lower part of the *punctata* Zone. The second and third T-R cycles cover the *punctata* and *hassi* sl Zones, the *jamieae* Zone and the major part of the Early *rhenana* Zone. The fourth cycle (superimposed by a few minor cycles) starts in the early *rhenana* Zone and continues till the *triangularis* Zone. The first, second and fourth cycles are considered eustatic. Through graphic correlation of the Composite Standard (CS) of the Frasnian (KLAPPER, 1997) with the regional composite of the Ardennes, new data are added to the CS of the Frasnian and some already incorporated ranges are extended.

Keywords: Frasnian, Ardennes, graphic correlation, T-R-cycles, conodonts.

Résumé

Une corrélation à haute résolution de 10 coupes frasniennes en Ardenne belge a été réalisée en utilisant la méthode de Corrélation Graphique. Les extensions stratigraphiques mesurées de 85 espèces de conodontes, 48 espèces de coraux, 29 espèces de brachiopodes et 1 espèce de stromatoporoïde, présentes dans ces coupes, ont été réunies dans un cadre chonostratigraphique et une coupe composée régionale en Ardenne a été établie. Cette coupe composée fournit une plus grande résolution stratigraphique que la zonation traditionnelle à conodontes. Cela permet de diviser le Frasnien en 532 unités de temps standard dérivées d'une coupe de référence composée située au bord sud du Synclinorium de Dinant et complétée par une coupe dans le Massif de Philippeville, pour le sommet du Frasnien qui n'est pas exposé au bord sud du Synclinorium de Dinant (unités 332-532). La nature diachronique des ensembles sédimentaires ressort clairement de la corrélation basée sur des lignes d'équivalence de temps. La combinaison de ces ensembles et de la succession des biofacies à conodontes dans les coupes permet de reconnaître quatre grands cycles T-R de 3ième ordre 500.00y-5m.y.. Le premier, qui commence au sommet du Givetien (Zone à *falsiovalis* inférieure) continue jusque dans la partie inférieure de la Zone à *punctata*. Les deuxième et le troisième cycles couvrent les Zones à *punctata*, à *hassi* sl, à *jamieae* et la plus grande partie de la Zone à *rhenana* inférieure. Le quatrième cycle (comprenant quelques cycles mineurs) commence dans la Zone à *rhenana* inférieure et continue jusque la Zone à *triangularis*. Les premier, deuxième et quatrième cycles sont considérés comme des cycles eustatiques. En corrélant la Coupe Composée Standard du Frasnien (KLAPPER, 1997) avec la Coupe Composée Régional en Ardenne, des données nouvelles sont ajoutées à la première et quelques extensions sont étendues.

Mots-clefs: Frasnien, Ardenne, corrélation graphique, cycles T-R, conodontes.

Introduction

During the last decades the taxonomy and stratigraphic distribution of Frasnian conodonts, corals, stromatoporoids and brachiopods from the Ardennes have been discussed in several papers. Most of these studies are geographically restricted or only considering part of the Frasnian. The aim of this study is to gather all these data, interpret them stratigraphically using the Graphic Correlation method and reconstruct the conodont biofacies evolution during the Frasnian as part of the basin history of the Ardennes. The conodont faunas used in the present study have been reviewed in order to obtain a uniform taxonomic approach. We follow the formational terminology and definitions recently revised by the Belgian National Subcommission on Devonian Stratigraphy (BOULVAIN *et al.*, 1999). The reader should refer to this paper for history of previous work.

Geological setting

FRASNIAN PALAEOGEOGRAPHY AND FACIES PATTERNS

During the Upper Devonian, the Ardennes region was situated in the subtropic regions of the Southern Hemisphere, and constituted a shelf area of the Old Red Continent. The Frasnian deposits of the Ardennes are transgressive to the N and NE of the Ardennes and are characterised by an extended carbonate buildup development.

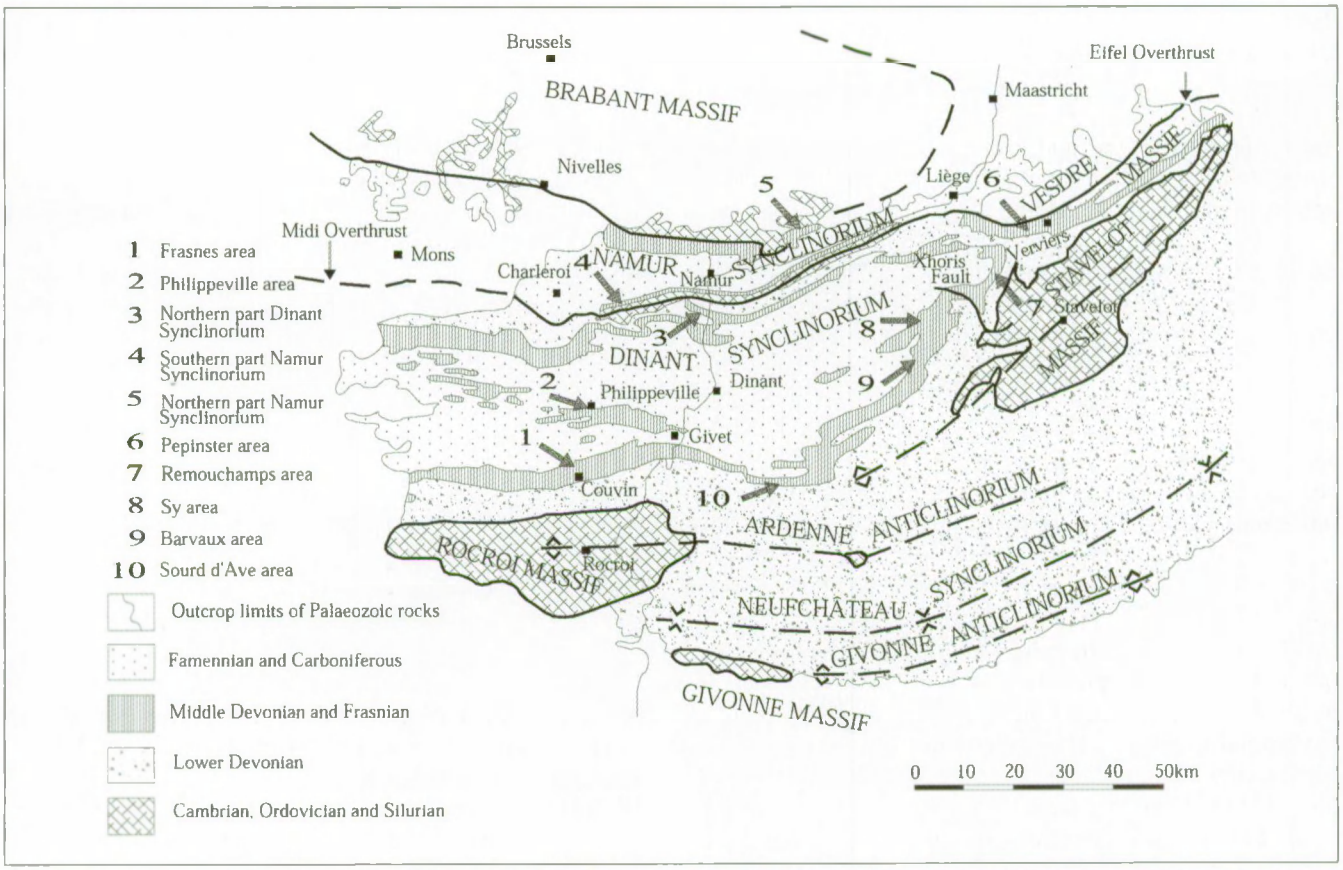

Fig. 1 — Geological setting and localisation of the studied sections

Three phases of reef building can be distinguished. The first two phases, which are characterised by the development of bioherms and biostromes, can be associated with relatively stable tectonic conditions. The third phase, with the formation of red mudmounds, is associated with a transgressive phase. In the deeper, southern part of the Ardennes, the reef facies are separated by shale deposits while in shallower waters, in the north, platy limestones were formed with less or without shale intercalations.

DATA

Our database consists of 10 mostly composite sections (Figs. 1, 16, 17), spread over the different structural units of the Ardennes, all of which contain a complete Frasnian succession. Some of the sections were assembled from several isolated outcrops; others (southern and northern part of the Namur Synclinorium) are from continuous outcrops. All data, except for the Frasnes railway section, have been taken from literature and include occurrences of conodonts, brachiopods, corals, stromatoporoids and bentonite layers. The conodont collection of COEN (1974) has been reviewed to obtain uniform taxonomic approach. The stratigraphic distribution of the most important Frasnian brachiopods and corals has been summarized in BOULVAIN *et al.* (1999).

1. The Nismes-Frasnes area in the southern part of the Dinant Synclinorium (BULTYNCK & JACOBS 1982; BULTYNCK *et al.* 1988; VANDELAER, *et al.*, 1989; SANDBERG *et al.*, 1992; BULTYNCK *et al.*, 1998). This section is assembled from 9 outcrops. The basal part of the Frasnian (Nismes Formation), studied at Nismes, is composed of greenish shales with nodular limestone at the base. The Moulin Liénaux Formation consists of a bedded limestone unit (Chalon Member), a reef unit (Arche Member) and shales (Ermitage Member), which occur above and lateral to the reef. The overlying Grands Breux Formation was studied in the Frasnes area. It has also a basal limestone unit (Bieumont Member) and shales (Boussu-en-Fagne Member) above and lateral to a reef unit (Lion Member). The upper part of the Frasnian, except for the top, has been examined in Nismes and Frasnes. It includes the Neuville Formation with nodular limestones, a red limestone layer (± 5m above the base of the formation in the acces road of the Lion quarry) and local red mudmounds, the Valisettes Formation with fine greenish shales and reduced to a few meters and the Matagne Formation with fine blackish shales and dark limestones in the basal part.

2. The Sourd d'Ave area in the eastern part of the southern border of the Dinant Synclinorium (BULTYNCK, 1974; COEN, 1977; BULTYNCK & JACOBS, 1982; BOUHARRAK, 1984; BULTYNCK *et al.*, 1988 and COEN oral information). Shales largely represent the Frasnian deposits in

this area. Nodular limestones and shales occur in the Nismes, the Moulin Liénaux, the Grands Breux and the Neuville Formations. Bedded limestones represent the Chalon and the Bieumont Members. According to COEN (oral information) the nodular limestone beds described by BOUHARRAK (1984) as the Chalon Member, actually belong to the Ermitage Member. The exposed part of the Upper Frasnian, consists of blackish Matagne Shales with nodular limestones at its base.

3. The Philippeville area in the western central part of the Dinant Synclinorium (COEN, 1978; BULTYNCK *et al.*, 1998). The Philippeville composite section contains data from 4 large outcrops. Two of them are situated in Philippeville (north and south) and two in Neuville (old and new railroad cut). In this area, the lower Frasnian Nismes Formation comprises shales and a few layers of limestone nodules. The overlying Pont de la Folle Formation is subdivided in the La Fontaine Samart Member consisting of limestones with a biostromal unit at its base and the Machenées Member with mainly shales and nodular limestone at the base. The Philippeville Formation consists entirely of limestone. The lower part comprises dark, thin bedded limestones, the upper 60m are a biostromal complex. The upper Frasnian Neuville Formation consists of nodular limestones and a red limestone layer (11m above the base of the formation); the Valisettes Formation is represented by greenish shales with nodular limestones in the upper part; the Matagne Formation is formed by fine dark shales with locally limestone beds at its base.

4. The northeastern part of the Dinant Synclinorium.
The Barvaux area (south of the Xhoris fault). This section is assembled from four large outcrops (COEN, 1974): Barvaux north and south, Durbuy and Aisne. It consists mainly of shale deposits (Nismes, Moulin Liénaux and Grand Breux Formations) with nodular and bedded limestones in the Ermitage, Chalon and Bieumont Members. The Neuville Formation is made up of shales containing limestone nodules. The fine shales of the Valisettes Formation with locally red mudmounds are reduced to about 25m. Violet shales of the Barvaux Formation overlie this formation.

The Sy area (south of the Xhoris fault). The succession in this area is based on outcrops at Sy, Verlaine, Tohogne, Septon and Sinsin (COEN, 1974; BULTYNCK & JACOBS, 1982). The Nismes Formation, containing shales, is thinner than in the Barvaux area. The overlying Philippeville Formation is a limestone unit composed of two biostromes, separated by a shale horizon. The Neuville Formation consisting of shales with limestone nodules, is thinner than in the Barvaux area. The fine shales of the Barvaux Formation contain red mudmounds.

The Remouchamps area (north of the Xhoris fault). The data are taken from four outcrops (COEN 1974): Aywaille, Remouchamps, Louveigne and Comblain-la-Tour. In the lower part, the succession is similar to that of the Sy area. The Aisemont Formation, well exposed in Aywaille, consists of shales with a few limestone layers and an upper part of nodular limestones. The overlying Lambermont Formation contains shales with a few limestone nodules.

5. The northern part of the Dinant Synclinorium (TSIEN *et al.*, 1973; COEN-AUBERT & COEN, 1974).
To compose this succession, 7 outcrops were analysed. The main outcrop is the quarry in Tailfer from which the Presles Formation and the Lustin Formation were described. These formations were also studied at Lustin, Godinne, Hun, Fidevoye and Bauche. The Presles Formation comprises at its base organoclastic limestone, containing a few horizons with hematitic oolithes. The remaining part of the formation is fine green shale. The lower part of the Lustin Formation is mainly built up of biostromal limestone, the upper half of fine dark limestones. The Aisemont Formation contains nodular limestones at its base, the main part consists of shales and the upper part is made up of massif limestone beds. The overlying shales with a few lumachelles and sandy shales near the top, represent the Lambermont Formation.

6. The southern part of the Namur Synclinorium.
The data for this area are from the Aisemont section (LACROIX, 1974), on which also the data from an outcrop in Huy (Statte) (COEN-AUBERT & LACROIX, 1979) are projected. The basal part of the Frasnian is represented by the Presles Formation comprising nodular limestones with oolitic hematite, overlain by shales. The Lustin Formation consists mainly of micritic limestone with a few thick biostromal layers. The Aisemont Formation is made up of nodular limestones overlain by shales and dolostones. The top of the Frasnian is represented by the shaly Lambermont Formation.

7. Northern part of the Namur Synclinorium. The selected succession is situated at Huccorgne, north-west of Huy, and consists of the Bovesse Formation, micritic limestones alternating with dolostones, the Huccorgne Formation, coral- and brachiopod-bearing limestones and the Aisemont Formation. The lower part of the latter consists of bedded limestones that can be distinguished from the Lustin Formation by its much more argillaceous character, the middle part contains mainly shales with some limestone nodules and the upper part of the Aisemont Formation is made up of dolostones (LACROIX, 1972; COEN-AUBERT & LACROIX, 1985).

8. The Vesdre Massif. The data are gathered from five outcrops: Pepinster, Renoupré, Surdents, Bellevaux and Nasproue (AUBERT, 1968; COEN-AUBERT, 1970; COEN-AUBERT, 1974). A very thin layer of hematitic ooliths represents the Presles Formation here. The Lustin Formation includes bioclastic limestones with a few shale intercalations. The Aisemont Formation comprises shales with nodular limestone layers. The Lambermont Formation consists of shales with limestone nodules.

Methods

The procedure used to correlate the Frasnian sections of the Ardennes is the graphic correlation method. Briefly,

this method starts with assembling stratigraphic data from measured and stratigraphically overlapping sections. Two of these sections are placed at right angle to form the axes of a x-y graph. The biostratigraphic data are represented by the first and last occurrences of each species, which are indicated as points on the graph. Through these points, a correlation line is drawn; this is the most important step in the graphic correlation method. The line of correlation (LOC) allows us to project stratigraphic events from one section into another. By correlating all our sections with one of them (the thickest and best-sampled one, which is also the most complete), the standard reference section (SRS), we can construct a regional composite , which contains all data from this region and estimate the total species ranges. The scale of the regional composite is divided in units derived from the original thickness of the standard reference section. These units can be projected onto the different sections to obtain time equivalent points, which can be used for a time correlation between two sections.

For graphic correlation of the Frasnian sections, we used a software program (Graphcor 3.0) for PC developed by Kenneth HOOD (1998). The Nismes-Frasnes section situated in the southern part of the Dinant Synclinorium (SSD) has been chosen as standard reference section because it is the most intensively studied one, the sampling intervals are generally small and it does not show any significant gaps or unconformities. The line of correlation was placed in a way that the bases and tops of the species were split in order to minimize the disruption of established ranges (''method of economy fit'') and along the greatest density of conodont events, mainly with respect to the first occurrence data. Because the conodonts can be reworked, we consider the first occurrence data more reliable. The 9 other sections were correlated with the standard in the following order: the Philippeville Massif (MPH), the Sourd d'Ave area (SA), the Barvaux area (SX2), the Sy area (SX1), the northern part of the Namur Synclinorium (NSN), the northern part of the Dinant Synclinorium (NSD), the Vesdre Massif (VM), the southern part of the Namur Synclinorium (SSN) and the Remouchamps area (NX). This procedure was repeated in rounds until the position of the lines of correlation was stabilised, in this study 9 rounds.

At this stage the composite section includes the maximum species ranges. Because we correlated these 10 sections, each containing a different thickness of sediments deposited during the same time interval, the scale of the composite standard section can no longer be seen as a thickness scale but should be used as a nonannual time scale. This scale is then divided into composite standard units (CSU), in the present study 532 composite standard units.

Results of the Graphic Correlation

Among the conodont ranges assembled in the Ardenne Regional Composite, the SSD section and the MPH section control the majority of the biostratigraphic data. The LOC of the latter (Fig. 4) intersects with the bases of the following species: *Ancyrodella alata, Ad. rugosa, Ad. lobata, Ad. curvata* (early), *Ad. curvata* (late), *Ancyrognathus triangularis, Palmatolepis triangularis* and *Macgeea rozkowskae* (rugose coral). A few other biostratigraphic events are located on or near the LOC. Unfortunately, due to a less dense sampling and the presence of a thick sequence with stromatoporoid beds barren of conodonts, a lot of bases lie 230m above the base of the MPH section near the top of the Philippeville Formation. This means that the first occurrences of these species (*Ancyrognathus coeni, Ag. tsiensi, Palmatolepis jamieae, Pal. proversa* and *Pal. hassi* s.l. a.o.) are probably lower in the section than now recognised. Apart from the base and the top of the section, the LOC in the graph of the Sourd d'Ave region (Fig. 5) is not controlled by many conodont events. Here we locate the LOC following the bases of a few stratigraphic important conodont species. The LOC of the NSN section with the CS gives a good separation of tops and bases and is divided into 7 components (Fig. 12). The correlation line is put through the bases of the rugosan taxa *Macgeea rozkowskae, Hexagonaria mirabilis, Argutastrea lecomptei, Wapitiphylum vesiculosum*, and *Phillipsastrea ananas ananas*. Six segments can be detected in the LOC of the NSD area (Fig. 9), going through the bases of *Ancyrodella alata, "Alveolites suborbicularis", "Amphipora pervesiculata", "Stromatopora goldfussi"* and *Phillipsastrea ananas ananas*. The position of a few bases that lie on the right side of the LOC (180-200) can be explained by poor sampling in the biohermal Arche Member of the SRS. Coral data are used to draw the correlation line of the Vesdre area (Fig. 10) by lack of sufficient conodont data. The graph of the SSN section with the Ardenne Regional Composite (Fig. 11) is defined by the bases of *Eodmitria oblivialis, "Alveolites suborbicularis", "Disphyllum rugosum", Hexagonaria mirabilis, Argutastrea koninckі, Wapitiphylum vesiculosum* and *"Cyrtospirifer monticolaformis"*. Six LOC segments can be located on the plot of the Remouchamps area and the CS (Fig. 8). Here we can observe a rather good separation of tops and bases. The graphs of the remaining sections (Figs. 6 and 7) are splitting the tops and bases rather well so that in these cases, the events cause no changes in range (with the exception of four coral events).

Plotting all sections against the Ardenne Regional Composite, significant differences in sediment accumulation rate are visible (Fig. 18). Evidence for synsedimentary tectonic events can be observed in the Barvaux area, for instance were we observe a higher sediment accumulation rate (CSU 310-320) than in the other regions. For the Lower and Middle Frasnian, we can observe a decrease in thickness from south to north (Figs. 16 and 17).

→

Fig. 2 — Composite standard conodont ranges of the Ardennes.

FAM.
triangularis
linguiformis
Late rhenana
Early rhenana
jamieae
hassi sl
punctata
transitans
Late falsiovalis
Early falsiovalis
late
early
FRASNIAN
middle
GIV
550
500
450
400
350
300
250
200
150
100
50
0
Uchtospirifer "orbelianus"
Desquamatia (Seratrypa) pectinata
Desquamatia (Seratrypa) suppinguis
Desquamatia (Neatrypa) gosseleti
Desquamatia (Neatrypa) europaea
Geminisulcispirifer bisinus
Metabolipa greindli
Plionoptycherhynchus exformosus
Hypothyridina cuboides sl
Eodmitria oblivialis
Desquamatia (Seratrypa) frasniense
Subquadriangulispirifer malaisi
Costatrypa fossae
Costatrypa icomptei
Apousiella bouckardi
Costatrypa variabilis
Neometabolipa delhayei
Desquamatia (Desquamatia) alticoliformis
Desquamatia (Desquamatia) quieta
Calvinaria megistana
"Minatothyris maureri"
Iowatrypa circuitonis
Neometabolipa duponti
Desquamatia (Seratrypa) derelicta
Iowatrypa rotundicollis
Spinatrypa tumuli
"Cyrtospirifer monticolaformis"
Rhyocarinynchus tumidus
"Stromatopora goldfussi"

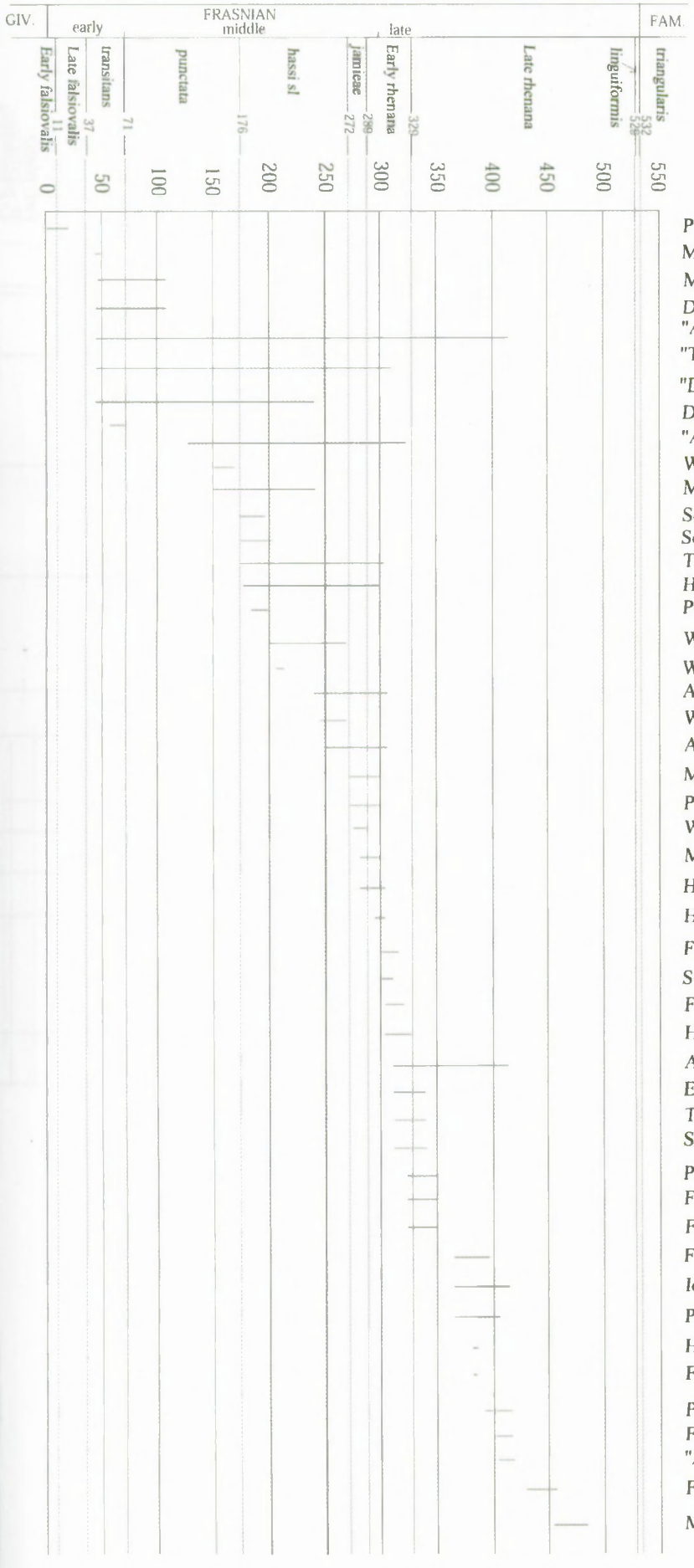

Phillipsastrea bouchardi
Macgeea multizonata
Macgeea rozkowskae
Disphyllum hilli
"Alveolites suborbicularis"
"Thamnopora boloniensis"
"Disphyllum goldfussi"
Disphyllum kostetskae
"Alveolites obtortus"
Wapitiphyllum soshkinae
Macgeea lacroixi
Scruttonia focantiensis
Scruttonia balconi
Tabulophyllum conspectum
Hexagonaria mirabilis
Peneckiella fascicularis
Wapitiphyllum irregulare
Wapitiphyllum tenue
Argutastrea konincki
Wapitiphyllum mahaniense
Argutastrea lecomptei
Macgeea gallica gallica
Peneckiella szulczewskii
Wapitiphyllum vesiculosum
Macgeea gallica gigantea
Hexagonaria mac
Hexagonaria davidsoni
Frechastraea phillipsastraeiformis
Scruttonia bowerbanki
Frechastraea carinata
Hankaxis insignis
Alveolites tenuissimus
Egosiella gracilis
Thamnopora micropora
Senceliaepora tenuiramosa
Phillipsastrea ananas ananas
Frechastaea pentagona micrastraea
Frechastraea limitata
Frechastraea pentagona pentagona
Iowaphyllum rhenanum
Phillipsastrea ananas veserensis
Hankaxis mirabilis
Frechastraea kaisini
Phillipsastrea hennahi falsa
Frechastraea pentagona minima
"Alveolites complanatus"
Frechastraea pentagona tunkanligense
Macgeea gallica pauciseptata

Exception is the northside of the Namur Synclinorium, where the deposits are thicker. For the Upper Frasnian, the thickness could indicate a subsidence in the Philippeville Massif and the northern part of the Dinant Synclinorium. In the SW-NE direction, we notice a decrease in thickness to the Northeast. The Middle and Upper Frasnian deposits in the Barvaux area are remarkably thicker than in the surrounding areas. The Barvaux area could lie on one of the NS orientated subsidence axes in the Frasnian (LECOMPTE, 1967).

The Ardenne Regional Composite subdivided into 532 composite standard units provides greater stratigraphic resolution for correlation than obtained by other methods. Unlike the traditional fashion of correlation, graphic correlation allows also a correlation of intervals in the sections in which the fossil record is very poor. By correlating sections with the composite standard, the amount of useful data of a section in the correlation increases, while in de traditional way of correlating a lot of data are not useful because they are only present in one of the two sections.

Uncertainty of the correlation

In order to estimate the uncertainty of the correlation, many factors, of which only some are measurable, have to be taken into account. The events commonly used in graphic correlation are the lowest and highest stratigraphic occurrences of the fossil taxa in the sections. Unfortunately, these events are only exceptionally the evolutionary first and last occurrences of the species. This is due to several causes e.g. the sampling density, fossil preservation, sample size, facies changes, migration of taxa. The true lowest local occurrence lies at or stratigraphically below the observed one and the highest true local occurrence lies always at or stratigraphically above the observed one. We take this into account by plotting the range endpoints as boxes in the graph (Figs. 13-15). The areas of the boxes reflect the intervals of uncertainty. The sides of the boxes represent ranges of the unsampled intervals, i.e. the interval between the lowest sample containing a fossil species and the next sample below, which does not contain the species, or the distance between the highest sample containing the species and the next higher sample without it. So the real local lowest and highest occurrences and therefore the correlation points lie somewhere in the boxes. Figs 13, 14 and 15 show the correlations of the sections with the

←

Fig. 3 — Stratigraphic ranges of corals, brachiopods and stromatoporoids in the Ardenne Regional Composite (GODEFROID, 1994, 1998, 1999; GODEFROID & HELSEN, 1998; GODEFROID & JACOBS, 1986; COEN, 1974, 1977; COEN & COEN-AUBERT, 1976; COEN-AUBERT, 1969, 1970, 1974, 1980a, 1980b, 1982, 1986a, 1986b, 1994, 1999; COEN-AUBERT & COEN, 1974; SARTENAER, 1999)

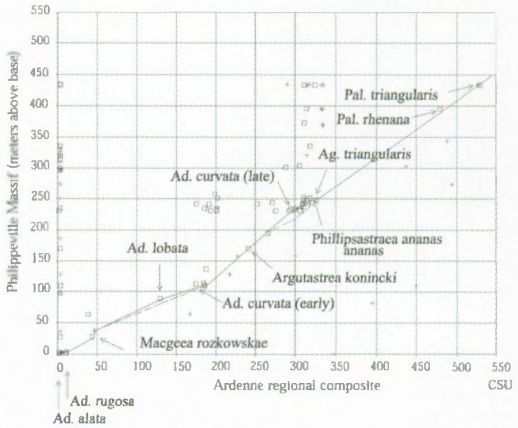

Fig. 4 — Graphic correlation of the Philippeville Massif composite section with the Ardenne Regional Composite. Indicated are the names of the most relevant taxa to draw the correlation line; □ first occurrence, + last occurrence.

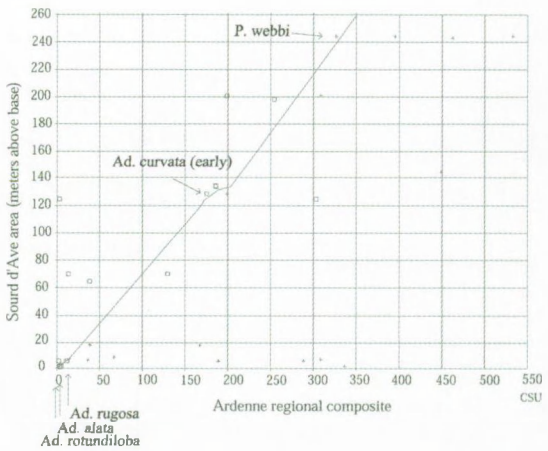

Fig. 5 — Graphic correlation of the Sourd d'Ave composite section with the Ardenne Regional Composite. See also Fig. 4.

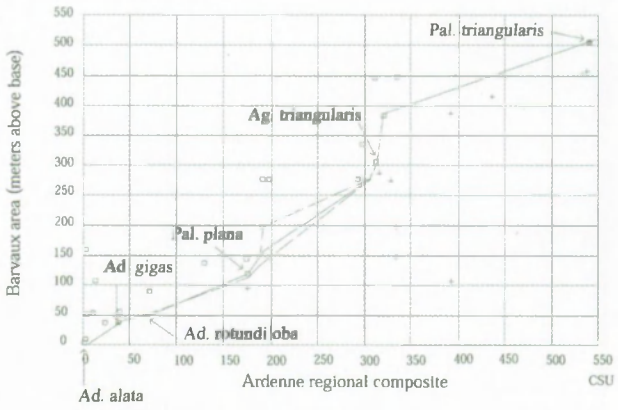

Fig. 6 — Graphic correlation of the Barvaux section with the Ardenne Regional Composite. See also Fig. 4.

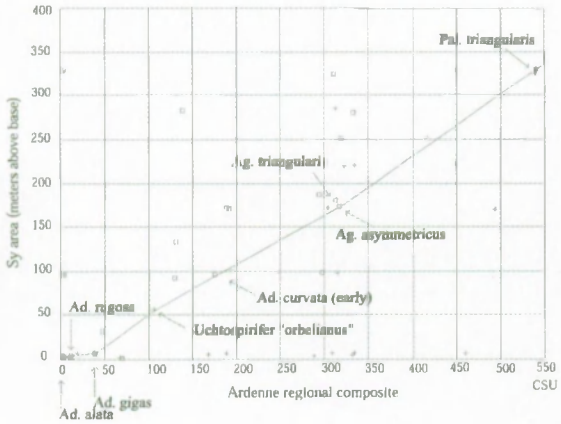

Fig. 7 — Graphic correlation of the Sy section with the Ardenne Regional Composite. See also Fig. 4.

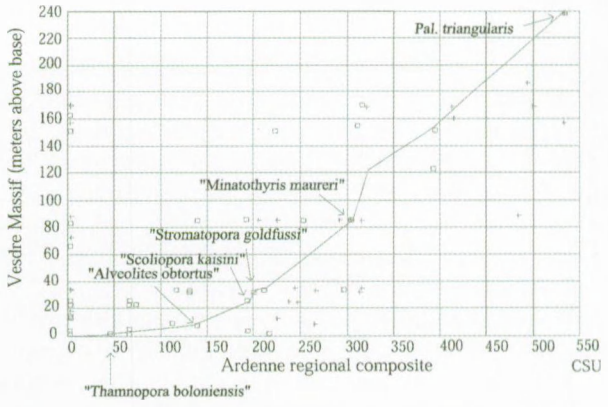

Fig. 10 — Graphic correlation of the Vesdre Massif composite section with the Ardenne Regional Composite. See also Fig. 4.

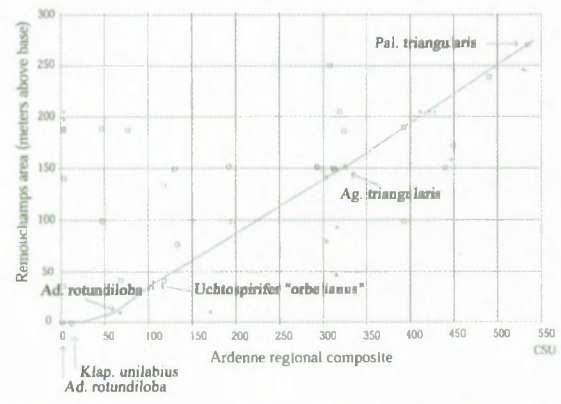

Fig. 8 — Graphic correlation of the Remouchamps section with the Ardenne Regional Composite. See also Fig. 4.

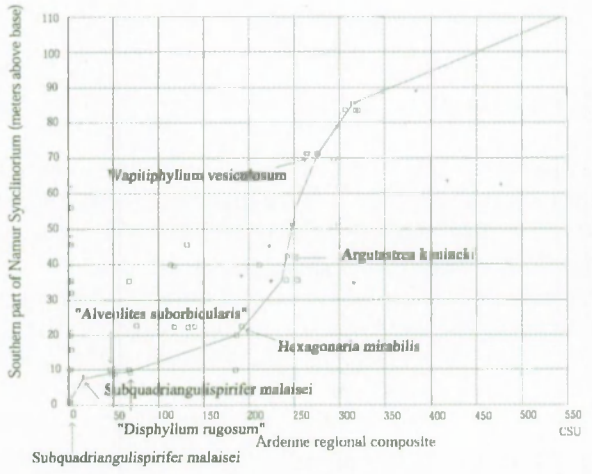

Fig. 11 — Graphic correlation of the composite section of the southern part of the Namur Synclinorium with the Ardenne Regional Composite. See also Fig. 4.

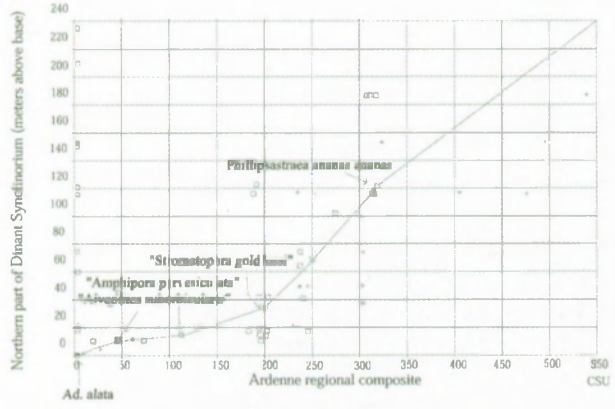

Fig. 9 — Graphic correlation of the composite section of the northern part of the Dinant Synclinorium with the Ardenne Regional Composite. See also Fig. 4.

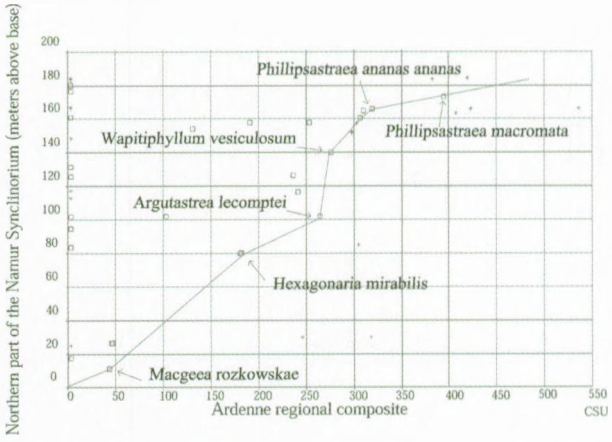

Fig. 12 — Graphic correlation of the composite section of the northern part of the Namur Synclinorium with the Ardenne Regional Composite. See also Fig. 4.

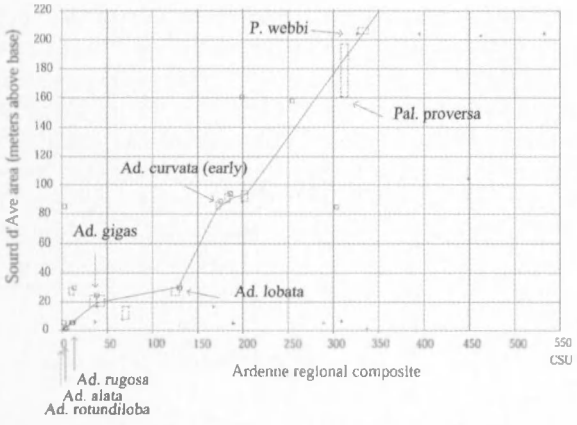

Fig. 13 — Correlation of the Sourd d'Ave composite section and the Ardenne Regional Composite, use of error boxes.

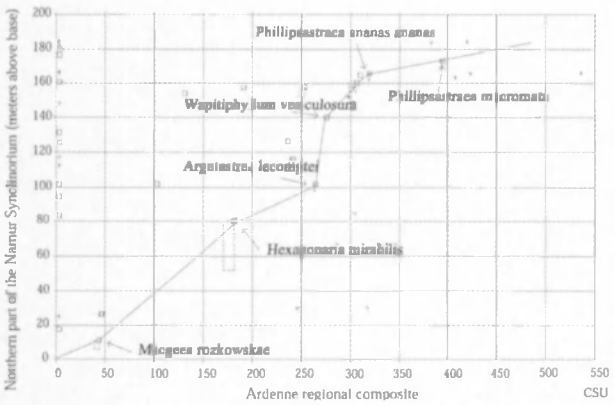

Fig. 14 — Correlation of the composite section of the northern part of the Namur Synclinorium and the Ardenne Regional Composite, use of error boxes.

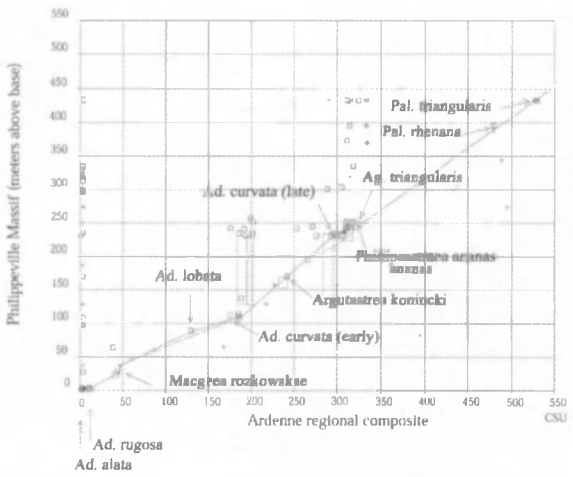

Fig. 15 — Correlation of the Philippeville Massif composite section and the Ardenne Regional Composite, use of error boxes.

largest boxes. The uncertainty calculated from these boxes represents only the error caused by the size of the sampling interval. Other causes like bad preservation, erosion or diagenetic processes cannot be calculated.

The uncertainty differs from place to place. In the correlation of the Sourd d'Ave section, the maximum uncertainty is 9%, indicated by the errorbox of *Palmatolepis proversa*. The maximum uncertainty in the correlation of the NSN section is 5%, indicated by the errorbox of *Hexagonaria mirabilis*. The correlation of the Philippeville Massif section shows a maximal error of 3%. In other cases the maximum uncertainty was even smaller.

Regional correlation

The regional correlation of the studied sections (Figs. 16 and 17) was obtained by projecting the composite standard units from the CS onto the particular sections. The time equivalent points were then used to correlate various sections together. Correlation lines were drawn every 50 units. Our results support previous correlations (COEN & COEN-AUBERT, 1971; COEN, 1973; COEN, 1974; BULTYNCK & JACOBS, 1982; COEN-AUBERT, 1982; BULTYNCK *et al.*, 1998; BOULVAIN *et al*, 1999) independent from previous interpretations.

Comparing the graphic correlation of the Frasnian with results of the lithostratigraphic correlation (BOULVAIN *et al.*, 1999), the diachronous nature of the lithologic units is obvious. Since the general correlation is shown in Figs. 16 and 17 only the important points of the study will be indicated here. The base of the Nismes-Presles Formation, for instance, becomes younger in northern direction. This trend is moreover associated with a progressive decrease in thickness.

The base of the first limestone member (Chalon Member in SSD, SA, SX2, Fontaine Samart Member in MPH, Lustin Formation in NSD, NX and SSN, the Philippeville Formation in SX1 and the Bovesse Formation in NSN) is slightly younger in northern and northeastern direction. The 50 CSU line is situated a few meters above the base of this limestone member in SSD, while in NDS, SSN, NX1 and SX1, it is located just beneath the base of the limestone member.

The same diachronous trend is recognised at the base of the second limestone member (Bieumont Member in SSD, SA and SX2, the Philippeville Formation in MPH, the second biostrome of the Lustin Formation in NX1 and the Huccorgne Formation in NSN). The base of the Bieumont Member is older than the base of the Philippeville Formation and the base of the second biostrome in the Lustin Formation in NX1. It has about the same age as the base of the Huccorgne Formation in NSN.

Through graphic correlation we find the base of the Neuville Formation time equivalent in all section were it is recognised and also very close to the base of the Aisemont Formation. On the other hand COEN (COEN *et al.*, 1976; BOULVAIN *et al.* , 1999) suggests that the base of the Neuville Formation (SSD, MPH, SX2 and SX1) is

clearly older than the base of the Aisemont Formation (NX1, VM, NSD, SSN and NSN), based on the first appearance of *Ancyrognathus triangularis* and the disappearance and appearance of respectively *Hexagonaria* and *Frechastrea* (corals). Correlation of MPH with NX1 based on these data indeed shows the difference in ages between the bases. Correlating MPH with SSD based on these data only, we would have to conclude that the base of the Neuville Formation is older in MPH than in SSD. However, graphic correlation of these sections (MPH and SSD), based on the first appearances of *Ancyrognathus curvata* (late), *Ag. asymmetricus, Ancyrodella nodosa* and *Ancyrognathus triangularis*, shows that the base of the Neuville Formation is time equivalent in both sections.

Through graphic correlation of all sections, we observe only a small difference (3 CSU) in time between the base of the Neuville Formation and the base of the Aisemont Formation. Taking into account the distance of 20 to 25km between the areas where the Neuville Formation is exposed and that characterized by the Aisemont Formation, we consider that the base Neuville Formation - base Aisemont Formation is only slightly diachronous.

Cyclicity

The evolution of conodont biofacies gives an indication of relative water depth during depositional time. For the present analysis only samples with 20 or more platform elements were taken into account. During the Famennian and most of the Frasnian, five biofacies belts have been recognised (SANDBERG & ZIEGLER, 1979; SANDBERG & DREESEN, 1984; SANDBERG *et al.*, 1988). The four outer biofacies belts each contained a single biofacies: palmatolepid, palmatolepid-polygnathid, polygnathid-icriodid and polygnathid-pelekysgnathid. The inner or fifth belt contained the polygnathid and the polygnathid-ancyrodellid biofacies during the Frasnian. During the early Frasnian Late *falsiovalis* and *transitans* Zones, when *Palmatolepis* was evolving from *Mesotaxis*, the five recognised biofacies belts were mesotaxid-polygnathid, polygnathid-icriodid, polygnathid-ancyrodellid, polygnathid and pandorinellinid. We also used the depth-stratification model of SEDDON & SWEET (1971), distinguishing two biofacies: the icriodid biofacies with mainly *Icriodus* and *Polygnathus* in a shallower-water layer, and the deeper palmatolepid biofacies. The biofacies found in the samples vary from the icriodid biofacies through polygnathid-icriodid, polygnathid, polygnathid-ancyrodellid, polygnathid-palmatolepid, and palmatolepid-polygnathid to palmatolepid and mesotaxid biofacies. A single genus name is given to samples that contain more than 75% of that genus. A double genus name is given to samples that contain more than 75% of those two genera together. Most analysed samples are from the southern part of the Dinant Synclinorium (Figs. 16,17). Deepening events are recognised in the Nismes Formation, the lower part of the Chalon Member, the Arche Member, within the upper part of the Ermitage Member, the lower part of the Bieumont Member, the Lion Member, the Neuville Formation, the Valisettes Formation and the Matagne Formation (SSD). A few small shallowing events are identified at the top of the Chalon Member, the top of the Arche Member, the top of the Ermitage Member, the top of the Boussu-en-Fagne Member, within the Neuville Formation, at the base of the Matagne Formation and in the upper part of the Lambermont Formation.

Relative water depth and T-R cycles can also be identified by lithological changes, combined with the diachronous character of lithological units.

1. Mudmounds / bioherms are considered to be built up during relative sea-level rises (Arche Member, Lion Member, mudmounds in the Neuville and Valisettes Formations). The carbonate productivity by reef builders is generally adequate to keep pace with rising sea level (BLOOM, 1974), (EMERY & MYERS, 1996, chapter 10: Carbonate Systems).
On the other hand, karstification at the top of the Lion Mudmound indicates a subareal exposure of the mudmound, taking place during a sea level fall.

2. Sedimentological study of the middle and upper part of the Philippeville Formation in MPH (DUMOULIN *et al.*, 1996) suggests a transgression in the middle part of the Philippeville Formation and a regression in the upper part (uppermost 20m).

3. Dark shales are often formed during transgressions (Matagne Formation). A high sea level favours increasing surface organic productivity in coastal waters and hence anaerobic conditions in the deeper water and on the sea floor (EINSELE *et al.*, 1991, chapter 5.1, Stratification in Black Shales: Depositional Models and Timing - an overview)

4. The diachronous shift of some deposits in the direction of the Devonian continent (northern direction) (the Pont d'Avignon Member, the bases of the Chalon Member and the Bieumont Member, the base of the Neuville/ Aisemont Formation and the Matagne Formation) (Figs. 16-17) indicates a transgression.

By combining these observations with the conodont biofacies, we can derive T-R cycles and project them onto the Standard Reference Section (SSD). The first transgression (diachronous nature of the Pont d'Avignon Member, shift from *Polygnathus-Icriodus* biofacies to *Polygnathus* biofacies) which already started in the latest Givetian, continues through the Nismes Formation and the Chalon Member. The first regression (transition from the *Polygnathus* biofacies to the *Polygnathus-Icriodus* biofacies) occurs near the top of this member. The second transgression (development of the Arche bioherm) starts

→

Fig. 16 — Correlation of the Frasnian sections in the south-eastern part of the Dinant Synclinorium and the Vesdre Massif.

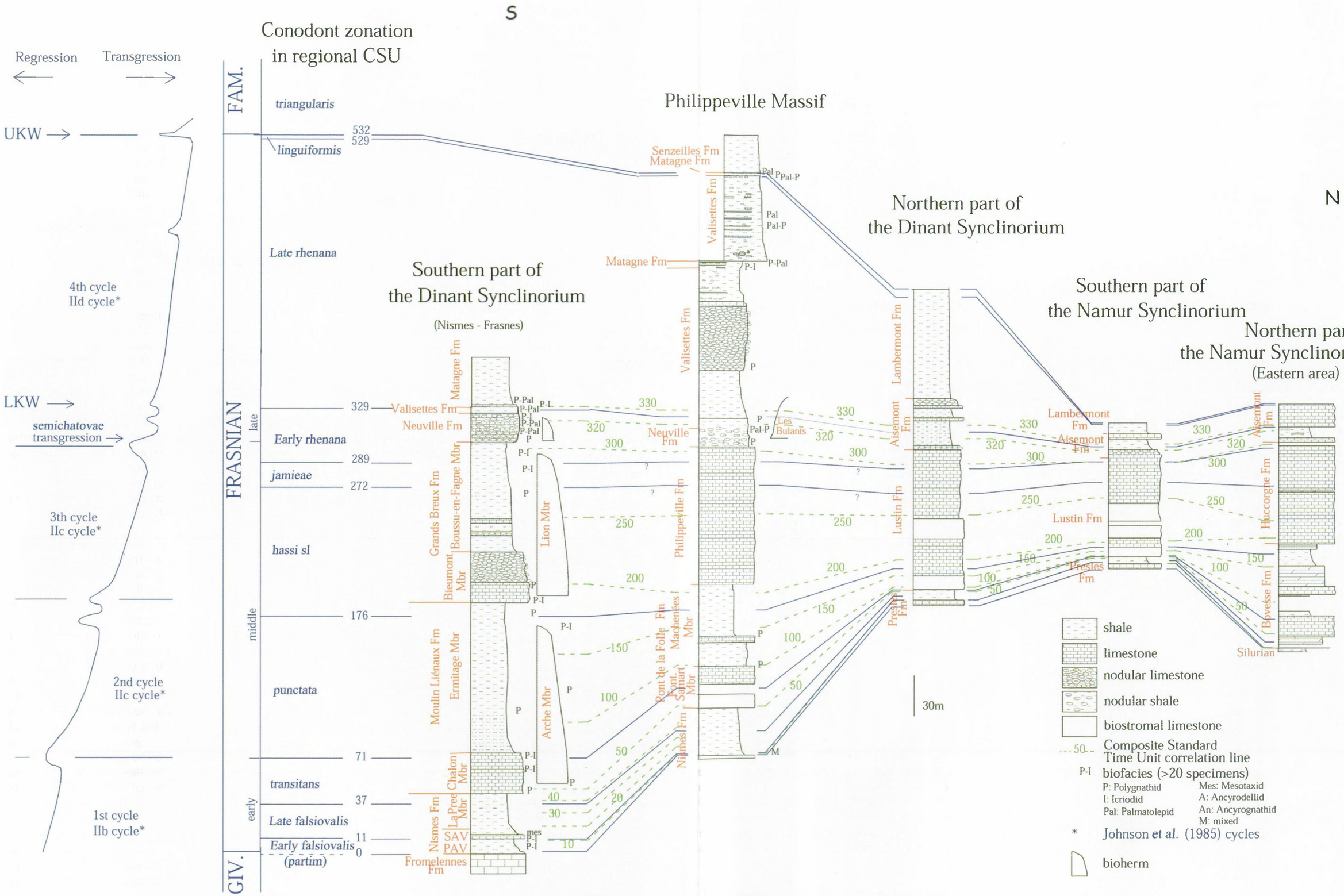
S
N
Regression
Transgression
Conodont zonation
in regional CSU
Philippeville Massif
Northern part of
the Dinant Synclinorium
Southern part of
the Dinant Synclinorium
(Nismes - Frasnes)
Southern part of
the Namur Synclinorium
Northern part of
the Namur Synclinorium
(Eastern area)
UKW
LKW
4th cycle
IId cycle*
semichatovae
transgression
3th cycle
IIc cycle*
2nd cycle
IIc cycle*
1st cycle
IIb cycle*
FAM.
FRASNIAN
GIV.
late
middle
early
triangularis
linguiformis
Late rhenana
Early rhenana
jamieae
hassi sl
punctata
transitans
Late falsiovalis
Early falsiovalis
(partim)
532
529
329
289
272
176
71
37
11
0
Senzeilles Fm
Matagne Fm
Valisettes Fm
Neuville Fm
Grands Breux Fm
Boussu-en-Fagne Mbr
Bieumont Mbr
Moulin Liénaux Fm
Ermitage Mbr
Chalon Mbr
La Pree Mbr
Nismes Fm
SAV
PAV
Fromelennes Fm
Lion Mbr
Arche Mbr
Philippeville Fm
Pont de la Folie Fm
Machenées Mbr
Pont Sanart Mbr
Nismes Fm
Les Bulants
Lambermont Fm
Aisemont Fm
Lustin Fm
Presles Fm
Huccorgne Fm
Boyesse Fm
Silurian
Pal
Ppal-P
P-Pal
P-I
P
Pal-P
M
Mes
330
320
300
250
200
150
100
50
40
30
20
10
?
30m
shale
limestone
nodular limestone
nodular shale
biostromal limestone
Composite Standard
Time Unit correlation line
biofacies (>20 specimens)
P: Polygnathid
I: Icriodid
Pal: Palmatolepid
Mes: Mesotaxid
A: Ancyrodellid
An: Ancyrognathid
M: mixed
Johnson et al. (1985) cycles
bioherm

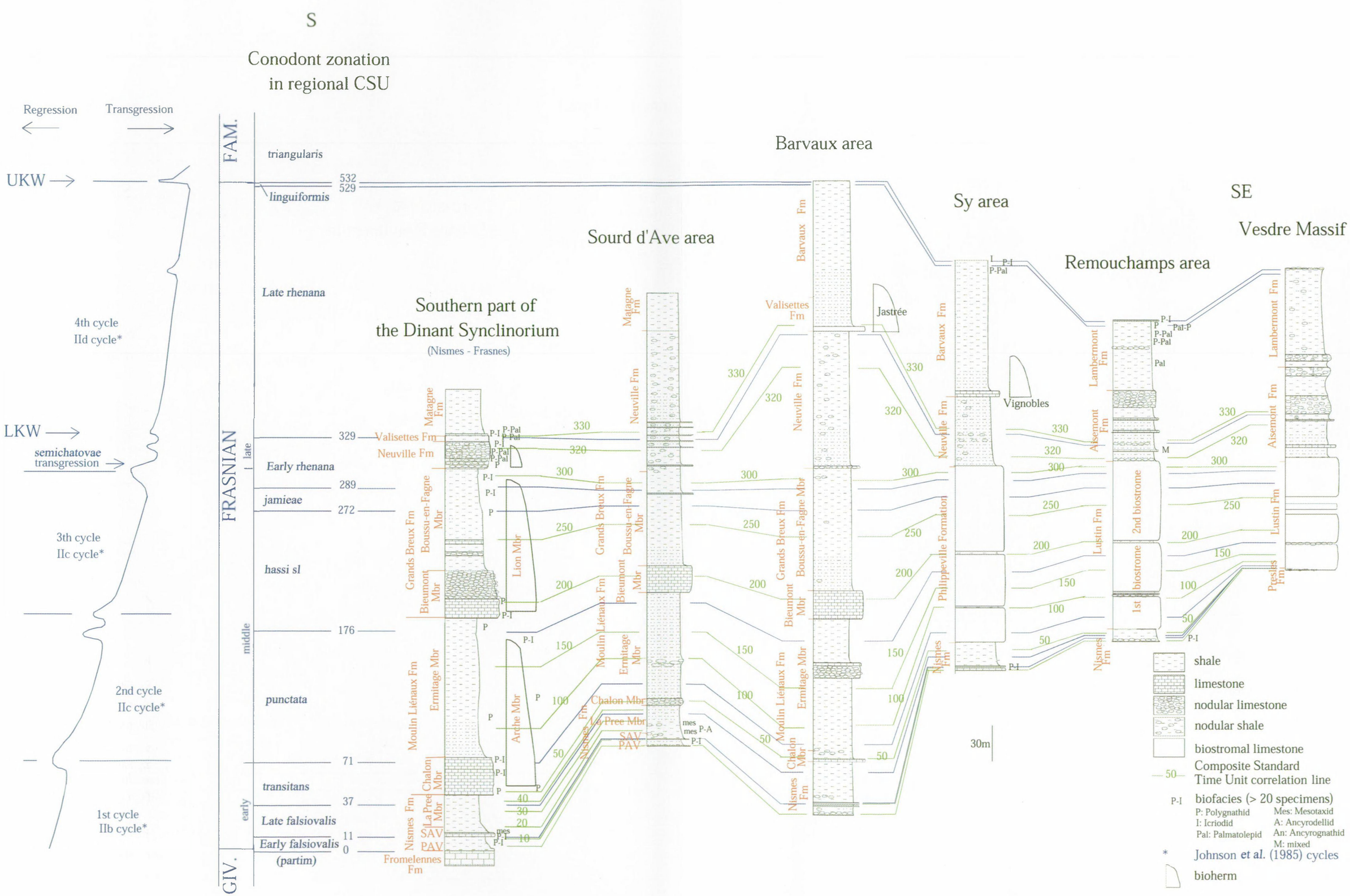
S
Conodont zonation
in regional CSU
Regression
Transgression
UKW
LKW
semichatovae
transgression
4th cycle
IId cycle*
3th cycle
IIc cycle*
2nd cycle
IIc cycle*
1st cycle
IIb cycle*
FAM.
FRASNIAN
GIV.
triangularis
linguiformis
Late rhenana
Early rhenana
jamieae
hassi sl
punctata
transitans
Late falsiovalis
Early falsiovalis
(partim)
532
529
329
289
272
176
71
37
11
0
late
middle
early
Barvaux area
Sy area
SE
Vesdre Massif
Sourd d'Ave area
Remouchamps area
Southern part of
the Dinant Synclinorium
(Nismes - Frasnes)
Matagne Fm
Neuville Fm
Valisettes Fm
Barvaux Fm
Jastrée
Vignobles
Philippeville Formation
Grands Breux Fm
Boussu-en-Fagne Mbr
Bieumont Mbr
Lion Mbr
Moulin Liénaux Fm
Ermitage Mbr
Archie Mbr
Chalon Mbr
La Pree Mbr
Nismes Fm
SAV
PAV
Fromelennes Fm
Lambermont Fm
Aisemont Fm
2nd biostrome
1st biostrome
Lustin Fm
Presles Fm
P-I
P-Pal
Pal
Pal-P
P
I
mes
P-A
330
320
300
250
200
150
100
50
40
30
20
10
30m
shale
limestone
nodular limestone
nodular shale
biostromal limestone
Composite Standard
Time Unit correlation line
biofacies (> 20 specimens)
P: Polygnathid
I: Icriodid
Pal: Palmatolepid
Mes: Mesotaxid
A: Ancyrodellid
An: Ancyrognathid
M: mixed
Johnson et al. (1985) cycles
bioherm

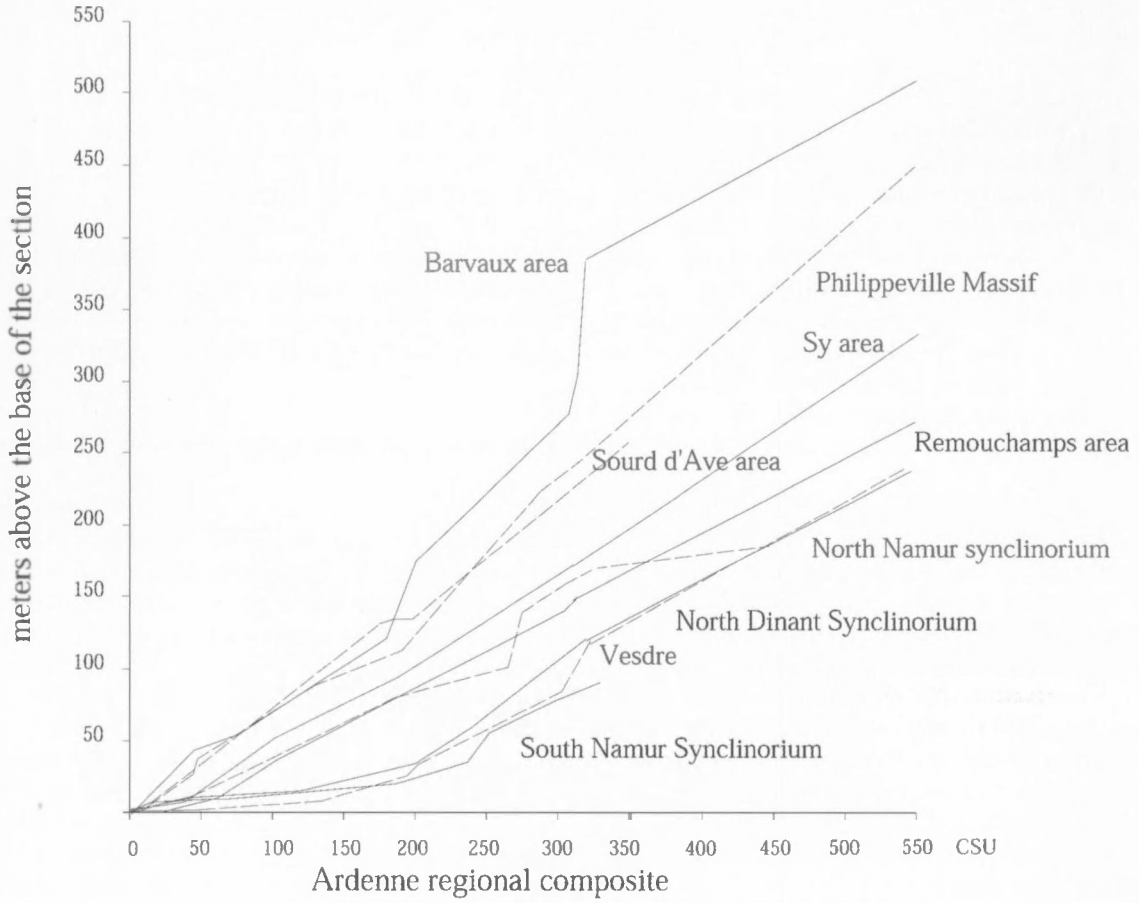

Fig. 18 — Comparison of graphs of the studied sections (plotted against the Ardenne Regional composite).

near the base of the Ermitage Member. This member ends with a small regression and a small T-R cycle (changing biofacies). The third major transgression (diachronous nature of the Bieumont Member, development of the Lion bioherm, sedimentology of the middle part of the Philippeville Formation) begins in the lower part of the Bieumont Member and continues up to the upper part of the Lion Member. In the uppermost part a small regression can be recognised (karstification of the top of the Lion bioherm, biofacies shift from *Polygnathus* to *Polygnathus-Icriodus* biofacies, sedimentology of the upper part of the Philippeville Formation). The fourth major transgression (slightly diachronous nature of the Neuville/ Aisemont Formation, development of mudmounds, conodont biofacies) starts at the base of the Neuville Formation and continues into the Matagne formation. This transgression (evolution from *Polygnathus* to the deep *Palmatolepis* biofacies, what makes it the deepest facies during Frasnian time) is interrupted by a few small regressions in the Neuville Formation and near the base of the Matagne Formation (conodont biofacies changes).

←

Fig. 17 — Correlation of the Frasnian sections from south to north.

The T-R cycles can be dated by conodonts. The first transgression, starting in the Early *falsiovalis* Zone, continues in the Late *falsiovalis* Zone and the *transitans* Zone. A small regression occurs just before the *punctata* Zone. The main part of this Zone corresponds to a second large transgression. The Zone ends with a small T-R-cycle. The *hassi sl* Zone starts with a small regression and continues during the third large transgression. This transgression ends in the *jamieae* Zone. A small regression separates it from the fourth large transgression (*semichatovae* transgression Early *rhenana* Zone). This transgression covers the whole Late *rhenana* Zone and is interrupted by a few small regressions. A new regression starts within the *linguiformis* Zone (shift from *Palmatolepis-Polygnathus* to *Polygnathus* biofacies, extinction of conodont species that were present in the Late *rhenana* zone). At the top of this zone we also recognise a transgression (shift from *Polygnathus* to *Palmatolepis* biofacies, beginning of new conodont species, Fig. 2).

Comparison of the T-R cycles of the Ardennes with the global T-R chart (JOHNSON, KLAPPER & SANDBERG, 1985)

The Frasnian T-R cycles of JOHNSON *et al.*, 1985 show

three major transgressive pulses from the latest Givetian to the late Frasnian (the bases of cycles IIb, IIc and IId). They correspond with the first, the second and the fourth transgressive pulse in the Ardennes. They can be considered as eustatic while they are also recognised in the New York area and Western Canada and, only for the fourth pulse, in Germany and the Western U.S. The transgression that starts in the lower part of the Late *rhenana* Zone (lower part of the Matagne shale in SSD) would agree well with the Lower Kellwasser event (BULTYNCK *et al.*, 1998). The Upper Kellwasser event was recognised (SANDBERG *et al.*, 1988) at Hony in the Lambermont Formation of the eastern part of Dinant Synclinorium (*linguiformis* Zone) and at the base of the Matagne Formation in the Philippeville Massif (BULTYNCK *et al.*, 1998).

SANDBERG *et al.* (1992) drew a T-R chart of the Middle Frasnian and the Early Fammenian in the Ardennes. A few differences are noticed when compared to our T-R chart. The base of the *jamieae* Zone is situated above the top of the Lion Member, whereas in our chart, the *jamieae* Zone starts in the Lion Member. The Late *rhenana* Zone starts in the Neuville Formation while in our chart it only starts in the Valisettes Formation, close to the top of the Neuville Formation. The LKW event corresponds with the base of the mudmound development within the Neuville Formation. We situate it in the lower part of the Matagne Formation (early Late *rhenana* Zone). The UKW event is recognised at the base of the Matagne Formation, where we position the LKW. We assign the UKW to the dark shale deposit above the upper part of the Valisettes Formation in the Philippeville Massif (BULTYNCK *et al.*, 1998). This difference is mainly due to an erroneous lithostratigraphic correlation between the deposits at Hony in which the *linguiformis* Zone was recognised by SANDBERG *et al.* (1988, p. 282; *"thin Matagne Shale equivalent") and the Matagne Shale in the southern part of the Dinant Synclinorium. Whereas this "thin Matagne Shale equivalent" at Hony only corresponds to the thin upper part of the Matagne Shale in the Philippeville Massif.*

The order of cyclicity of the Ardennes T-R cycles, may be recognised by comparing them to the duration of the conodont zones. TUCKER *et al.* (1998) propose a Devonian time scale based on newly determined U-Pb zircon ages of volcanic ashes, closely tied to biostratigraphic zones. They suggest a duration of 6 m.y. for the Frasnian. Projection of the Frasnian conodont zone boundaries on the time line (TUCKER *et al.*, 1998, fig. 2) provides an estimated duration of the Frasnian biozones (0.4 m.y. for the *linguiformis* Zone and the *jamieae* Zone, 2.4 m.y. for the *rhenana* Zone, 1.2 m.y. for the *hassi* Zone, 0.3 m.y. for the *transitans* Zone and 1.65 m.y. for the *punctata* Zone and the Frasnian part of the *falsiovalis* Zone). According to SANDBERG *et al.* (1988), the Lower *gigas* Zone (= Late *rhenana* Zone) may have been as long as 0.7 m.y., whereas the *linguiformis* Zone probably was as short as 0.3 m.y.. SANDBERG & ZIEGLER (1996) assume a 0.3 m.y. and 0.7 m.y. duration for the *jamieae* Zone respectively the Early *rhenana* Zone. In this paper, the durations of TUCKER *et al.* (1998) have been used.

Cycle II: 0.8 m.y. ($\pm$ 200.000y)
Cycle III: 1.94 m.y. ($\pm$ 600.000y)
Cycle IV: 2.3 m.y. ($\pm$ 800.000y)
Frasnian part of Cycle I:
0.95 m.y. ($\pm$ 400.000y)

These durations agree well with the duration of the 3rd order cycles (500.000y-5m.y.) of VAIL *et al.* (1991). The minor T-R cycles that are superposed to them are 4th order cycles (duration of 100.000y- 500.000y).

Composite standard range charts of the Ardennes

The conodont based Ardenne Regional Composite of the Frasnian constructed by graphic correlation of 10 sections is given in Fig. 2. This composite section includes also coral, brachiopod and stromatoporoid records (Fig. 3).

The Frasnian is subdivided into 532 composite standard units (CSU), derived from the thickness of the standard reference section (SSD), and provides a greater stratigraphic resolution for correlation in the Ardennes than any other stratigraphic method. The Frasnian CS reveals considerable differences in duration of the conodont zones (in composite standard units). Unit 0 is placed at the base of the Nismes Formation in our reference section and does not coincide with the base of a conodont zone. The base of the Frasnian, as defined by the first occurrence of *Ad. rotundiloba* in the Nismes section (BULTYNCK, 1982: pl. 1, figs. 26-27) is located at 1.8 CSU. The Early *falsiovalis* Zone is indicated by the presence of *Ancyrodella pristina*, *Ad. soluta* and *Ad. binodosa*. The limit between the Early *falsiovalis* and Late *falsiovalis* Zones is situated at 11 units, when *Ad. rugosa* makes its first appearance.

Mesotaxis asymmetricus enters somewhat higher in the zone. *Palmatolepis transitans* appears at unit 37, defining the base of the *transitans* Zone. The *punctata* Zone starts at CSU 71, the earliest occurrence of *Pal. punctata* and ranges till CSU 176 corresponding with the first occurrence of *Pal. hassi* s.l. and the early form of *Ancyrodella curvata*. The upper limit of the *hassi* s.l. Zone is defined by the first occurrence of *Pal. jamieae* at CSU 272. The appearance of *Pal. nasuta* indicates the start of the Early *rhenana* Zone at CSU 289. The Late *rhenana* Zone ranges from the first occurrence of *Pal. rhenana* (CSU 329) until the appearance of *Pal. linguiformis* (CSU 529). The Frasnian/Famennian boundary defined by the first occurrence of *Pal. triangularis* is recognised at CSU 532.

Table 1 shows the ranges of the conodont taxa and their occurrence in the studied sections. Most of the data are derived from the standard reference section (SSD) and from the Philippeville Massif. Most of the first and last occurrences did not need adjustments, as was shown by the graphic correlation of the sections, because the lowest first appearance and the highest latest occurrence were already documented in the standard reference section.

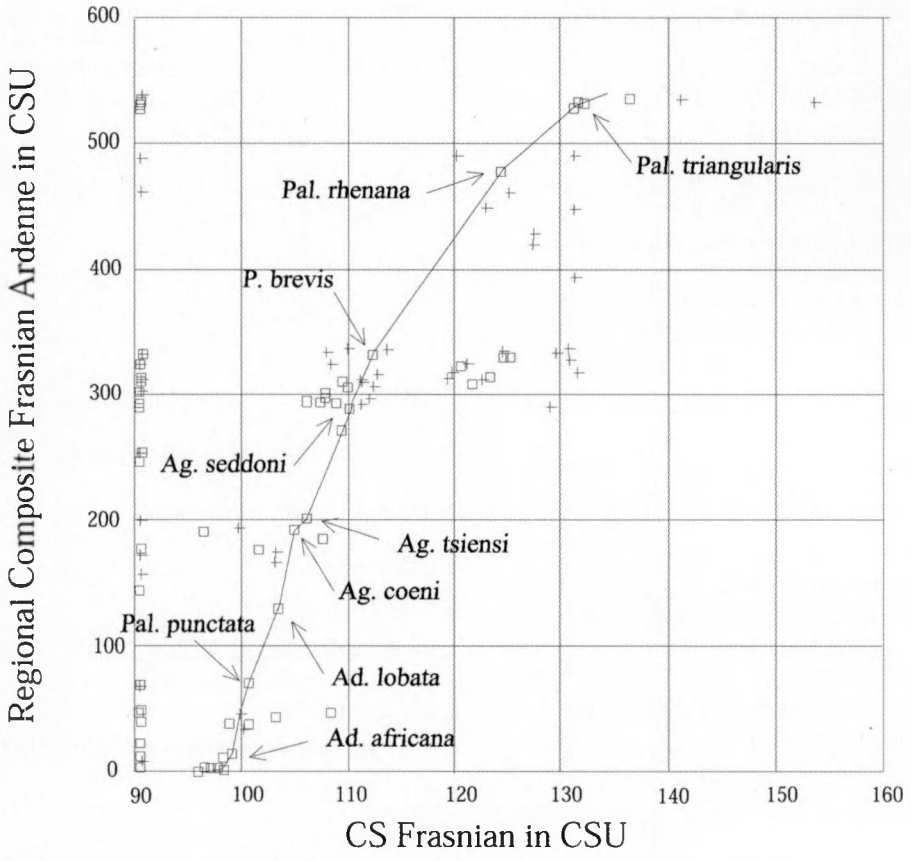

Fig. 19 — Correlation of the Ardenne Regional Composite with the Frasnian CS (KLAPPER, 1997).

Only 30% of the data were adjusted through graphic correlation.

The graphic correlation allows to mark the conodont zones in every studied section by projecting the zonal boundaries from the composite standard (Figs. 16 and 17), even in the sections where it was formerly impossible to recognised the conodont zones due to insufficient conodont data (NSD, SSN, VM, NSN, SX1, SX2, NX1). Furthermore, the graphic correlation allows to define more precisely the limits of some conodont zones, previously recognise in the Ardennes area. The lower limit of the Early *rhenana* Zone in the SSD is lowered compared to former publications (BOULVAIN *et al.*, 1999). In the MPH the base of the punctata zone can also be lowered and is positioned in the middle part of the Fontaine Samart Member.

Correlation of the CS of the Ardennes with the CS of the Frasnian

KLAPPER (1997) established a Frasnian composite standard by assembling data from the Montagne Noire and Western Canada. To correlate our regional composite with the Frasnian composite standard, we used graphic correlation (Fig. 19). The LOC was drawn by splitting the tops and bases. For the first 150 units of the Ardennes composite, the position of the LOC was rather clear. Between units 200-300, only few conodont data are available, due to the mostly unfavourable biohermal facies during this time interval. The consequence is that the first occurrences just beneath the 300 unit line might be found in older units, closer to the LOC line. After establishing the LOC, the information from the Ardenne Regional Composite can be projected onto the Frasnian composite standard. In this way, new data are added to the Frasnian composite and a few conodont ranges are extended (Table 1).

Systematic palaeontology

Representatives of the conodont genera *Ancyrodella, Ancyrognathus, Klapperina, Mesotaxis* and *Palmatolepis* from sections in the Ardennes that have not been photographically illustrated before (M. COEN collection) and some taxa that are mentioned for the first time from the Ardennes (e.g. *Palmatolepis domanicensis*) are figured in Plates 1-2. Synonymies are limited to the original reference of the taxon, to major revisions and to figured or quoted specimens from Frasnian sections in the Ardennes. They are necessary to make the link between our data and the conodont data of former publications.
All figured specimens are stored at the Institut Royal des Sciences Naturelles de Belgique, under catalogue numbers IRScNB N°b 3671- b 3697.

Genus *Ancyrodella* ULRICH & BASSLER, 1926

Ancyrodella africana GARCÍA-LÓPEZ, 1981
Pl. 1, Figs. 7-8.

1981 *Ancyrodella africana* n. sp. - GARCÍA-LÓPEZ, p. 264, pl. 1, figs. 1-4.
1974 *Ancyrodella rotundiloba* (BRYANT) - COEN, pl. 1, Sy section, unit a (partim).
1989 *Ancyrodella africana* GARCÍA-LÓPEZ, - VANDELAER, VANDORMAEL & BULTYNCK, pl. 1, figs. 6a, b & 7a, b.

Ancyrodella alata GLENISTER & KLAPPER, 1966

1966 *Ancyrodella rotundiloba alata* n. sp. - GLENISTER & KLAPPER, pp. 799-860, pl. 85, figs. 1-8, pl. 86, figs. 1-4.
1974 *Ancyrodella rotundiloba alata* GLENISTER & KLAPPER - COEN-AUBERT & COEN, p. 511.
1974 *Ancyrodella alata* GLENISTER & KLAPPER - COEN, pl. 4.
1978 *Ancyrodella rotundiloba* alata GLENISTER & KLAPPER - COEN, p. 26, fig. 3, unit a (partim).
1978 *Ancyrodella rotundiloba alata* GLENISTER & KLAPPER - BULTYNCK & JACOBS, tab. 1-2, pl. 2, figs. 4-8.
1985 *Ancyrodella alata* GLENISTER & KLAPPER - KLAPPER, pl. 4, figs. 1-8, pl. 5, figs. 1-16, pl. 6, figs. 1-12, pl. 7, figs. 1-11, pl. 8, fig. 8.
1989 *Ancyrodella alata* GLENISTER & KLAPPER - VANDELAER, VANDORMAEL & BULTYNCK, pl. 1, figs. 2a, b.

Ancyrodella binodosa UYENO, 1967

1967 *Ancyrodella rotundiloba binodosa* n. subsp. - UYENO, pp. 4-5, pl. 1, fig. 2, 4, 5.
1973 *Ancyrodella rotundiloba binodosa* UYENO - TSIEN, DRICOT, MOURAVIEFF & BOUCKAERT, p. 10.
1974 *Ancyrodella rotundiloba binodosa* UYENO - COEN-AUBERT & COEN, p. 511, pl. 1.
1974 *Ancyrodella rotundiloba binodosa* UYENO - COEN, p. 84.
1982 *Ancyrodella binodosa* UYENO δ morphotype - BULTYNCK & JACOBS, pl. 1, figs. 25, 28-30.

Ancyrodella curvata (BRANSON & MEHL, 1934)
Pl. 2, Figs. 1-6.

1934 *Ancyrognathus curvata* n. sp. - BRANSON & MEHL, p. 241, pl. 19, figs. 6, 11.
1974 *Ancyrodella curvata* (BRANSON & MEHL) - COEN, pp. 77, 81, 86, 91, 100, pl. 4.
1974 *Ancyrodella curvata* (BRANSON & MEHL) - COEN-AUBERT, p. 61.
1974 *Ancyrodella curvata* (BRANSON & MEHL) - COEN-AUBERT & COEN, pp. 516, 517, 520, 521.
1976 *Ancyrodella curvata* (BRANSON & MEHL) - COEN & COEN-AUBERT, pp. 2, 3, 4, 6.
1979 *Ancyrodella curvata* (BRANSON & MEHL) - COEN-AUBERT & LACROIX, p. 270.
1989 *Ancyrodella curvata* (BRANSON & MEHL) - VANDELAER, VANDORMAEL & BULTYNCK, pl. 3, figs. 1a, b.
1992 *Ancyrodella curvata* (BRANSON & MEHL) - ZANDBERG, ZIEGLER, DREESEN & BUTLER, tab. 1.
1998 *Ancyrodella curvata* (BRANSON & MEHL) - BULTYNCK, HELSEN & HAYDUKIEWICZ, pl. 5, figs. 8-10, pl. 6, figs. 1-3.

Ancyrodella gigas YOUNGQUIST, 1947
Pl. 1, Figs. 9-12.

1947 *Ancyrodella gigas* n. sp. - YOUNGQUIST, p. 96, pl. 25, fig. 23.
1974 *Ancyrodella gigas* YOUNGQUIST - COEN, pl. 4, pp. 78, 81, 83, 86, 89, 93, 96, 98.
1979 *Ancyrodella gigas* YOUNGQUIST - COEN-AUBERT & LACROIX, p. 276.
1984 *Ancyrodella buckeyensis* STAUFFER - BOUHARRAK, pp. 62, 66.
1985 *Ancyrodella gigas* YOUNGQUIST - KLAPPER, pl. 10, figs. 1-6, 9, 10, 13-16, text-fig 3EE-GG
1989 *Ancyrodella gigas* YOUNGQUIST - VANDELAER, VANDORMAEL & BULTYNCK, pl. 2, figs. 4a, b, 5a, b, 6a, b, 7.
1992 *Ancyrodella buckeyensis* STAUFFER - SANDBERG, ZIEGLER, DREESEN & BUTLER, tab. 1, 2.

Ancyrodella pristina KHALYMBADZHA & CHERNYSHEVA, 1970

1970 *Ancyrodella pristina* n. sp. - KHALYMBADZHA & CHERNYSHEVA, pp. 89-90, pl. 1, figs. 3-8.
1982 *Ancyrodella binodosa* UYENO α morphotype - BULTYNCK & JACOBS, pl. 1, figs. 19-21.
1982 *Ancyrodella binodosa* UYENO β & γ morphotypes - BULTYNCK, pl. 1, figs. 22-24.

Ancyrodella rotundiloba (BRYANT, 1921)
Pl. 1, Figs. 1-2.

1921 *Polygnathus rotundilobus* n. sp. - BRYANT, pp. 26-27, pl. 12, figs. 1-6.
1973 *Ancyrodella rotundiloba rotundiloba* (BRYANT) - TSIEN, DRICOT, MOURAVIEFF & BOUCKAERT, p. 10.
1974 *Ancyrodella rotundiloba* (BRYANT) - COEN, pl. 1,2,4, pp. 69, 72, 73, 83, 84, 96.
1974 *Ancyrodella rotundiloba rotundiloba* (BRYANT) - COEN-AUBERT & COEN, pp. 510, 511, 519.
1978 *Ancyrodella rotundiloba* (BRYANT) - COEN-AUBERT & LACROIX, p. 276.
1982 *Ancyrodella rotundiloba rotundiloba* (BRYANT) - BULTYNCK & JACOBS, pl. 1, figs. 26-27, pl. 2, figs. 1-3 (only), texttab. 1-2.
1985 *Ancyrodella rotundiloba* (BRYANT) - KLAPPER, only late form, pp 24-27, pl. 2, figs. 1-4, pl. 3, figs. 1-4,12, pl. 4, figs. 9-12, pl. 8, figs. 9, 10, pl. 11, figs. 3, 4, text-fig. 3E-J, M, N.
1989 *Ancyrodella rotundiloba* (BRYANT) - VANDELAER, VANDORMAEL & BULTYNCK, pl. 1, figs. 1a, b.

Ancyrodella rugosa BRANSON & MEHL, 1934
Pl. 1, Figs. 3-6.

1934 *Ancyrodella rugosa* n. sp. - BRANSON & MEHL, p. 239, pl. 19, figs. 15, 17.

Table 1 — Conodont taxa ranges and their occurrence in the studied sections. In the third and fourth column, the first and last occurrences of the species in the Ardenne Regional Composite are shown. The scale is given in regional composite units.

Nr	conodont species	First occurrence in Ardenne regional composite	Last occurrence in Ardenne regional composite	SSD	MPH	NSD	SSN	NSN	SA	SX2	SX1	NX	VM	First occurrence in Frasnian composite (Klapper, 1997)	Last occurrence in Frasnian composite (Klapper,1997)
1	Ancyrodella africana	01 3	131	+*	-	-	-	-	-	-	O	-	-	99.1	103.6
2	Ancyrodella alata	01.5	03 5	O	O	+	-	-	*	O	-	-	-	98.3	100.4
3	Ancyrodella binodosa	000	0 07	+	O	O	O	O		*	O	O	O	96.1	98.6
4	Ancyrodella curvata (early)	176	316	+	*	-	-	-	O	O	O	-	-	101.6	128.7
5	Ancyrodella curvata (early-late)	306	311	+*	-	-	-	-	-	-	-	-	-	111	121.9
6	Ancyrodella curvata (late/latest)	300	532	+	O	-	-	-	-	O	*	O	-	108	132
7	Ancyrodella gigas	03 8	324	*	O	O	-	-	O	O	+	-	-	100.4	112
8	Ancyrodella ioides	321	325	+*	-	-	-	-	-	-	-	-	-	111.7	121.1
9	Ancyrodella irregularis	310	310	+*	-	-	-	-	-	-	-	-	-	121.8	121.8
10	Ancyrodella lobata	130	449	+	O	-	-	-	O	*	O	O	-	103.6	123
11	Ancyrodella nodosa	294	393	+	O	-	-	-	-	O	*	O	-	107.6	131.3
12	Ancyrodella pramosica	01 3	04 7	+*	-	-	-	-	-	-	-	-	-	99.1	100.8
13	Ancyrodella pristina	000	0 03	+*	-	-	-	-	-	-	-	-	-	96.1	98.3
14	Ancyrodella rotundiloba	01.5	06 7	+	O	*	-	-	O	O	O	O	O	97.9	101.5
15	Ancyrodella rugosa	01 1	03 6	O	O	-	-	-	+	-	*	-	-	98.9	100.4
16	Ancyrodella soluta	01.5	0 04	+*	-	-	-	-	-	-	-	-	-	97.9	98.4
17	Ancyrognathus amana	309	327	+	-	-	-	-	-	-	-	*	-	111	130.6
18	Ancyrognathus ancyrognathoideus /primus	06 9	199	+*	-	-	-	-	-	-	-	-	-	100.8	106.0
19	Ancyrognathus asymmetricus	329	490	O	O	O	-	-	-	-	+	*	O	112.1	131
20	Ancyrognathus calvini	289	297	+*	-	-	-	-	-	-	-	-	-	110.3	110.6
21	Ancyrognathus coeni	192	316	+	-	-	-	-	-	O	*	-	-	105.2	112.7
22	Ancyrognathus seddoni	289	311	+*	-	-	-	-	-	-	-	-	-	110.1	122.0
23	Ancyrognathus sinelamina	532	532	-	+*	-	-	-	-	-	-	-	-	132.1	148.8
24	Ancyrognathus sinelobus	314	489	+	*	-	-	-	-	-	-	-	-	111.4	125.7
25	Ancyrognathus triangularis	309	420	+	-	-	-	O	-	-	-	-	*	109.5	127.4
26	Ancyrognathus tsiensi	199	449	+*	O	-	-	-	O	O	-	-	-	106.0	113.9
27	Ancyrognathus ubiquitus	529	532	-	+*	-	-	-	-	-	-	-	-	131.1	131.6
28	Icriodus alternatus alternatus	310	529	+	*	-	-	-	-	-	-	-	-	109.4	148.3
29	Icriodus alternatus helmsi	311	530	+	*	-	-	-	-	-	-	-	-	122.0	131.6
30	Icriodus cornutus	532	531	-	+*	-	-	-	-	-	-	-	-	131.4	131.8
31	Icriodus expansus	0(–)	309	+*	-	-	-	-	O	-	O	-	-	96.1	121.6
32	Icriodus latecarinatus	0 01	0 02	+*	-	-	-	-	-	-	-	-	-	97.0	97.9
33	Icriodus praealternatus	253	489	+	*	-	-	-	-	-	-	-	-	108.4	125.7
34	Icriodus subterminus	0 01	289	+*	-	-	-	-	O	-	O	-	-	96.5	128.8
35	Icriodus symmetricus	0 02	461	O	*	-	-	-	O	-	+	-	-	97.5	125.1
36	Klapperina ovalis	01 1	168	*	+	-	-	-	O	O	O	-	-	98.7	104.4
37	Klapperina unilabius	01 3	171	*	-	-	-	-	-	O	-	+	-	99.1	104.4
38	Mesotaxis asymmetricus	02 2	171	+*	-	O	-	-	-	O	-	-	-	99.3	104.4
39	Mesotaxis falsiovalis	03 9	172	*	-	-	-	-	-	+	-	-	-	99.7	104.4
40	Ozarkodina gradata	0 05	0 05	+*	-	-	-	-	O	-	-	-	-	98.4	98.5
41	Palmatolepis barba	296	302	+*	O	-	-	-	-	-	-	-	-	110.5	110.8
42	Palmatolepis brevis	290	293	+*	-	-	-	-	-	-	-	-	-	110.3	111.5
43	Palmatolepis delicatula	532	532	-	+*	-	-	-	-	-	-	-	-	132	136.1
44	Palmatolepis domanicensis	296	306	+*	-	-	-	-	-	-	-	-	-	107.9	112.5
45	Palmatolepis ederi	292	295	+*	-	-	-	-	-	-	-	-	-	109	111.9
46	Palmatolepis eureka	289	317	+*	-	-	-	-	-	-	-	-	-	110	111.5
47	Palmatolepis cf foliacea	292	295	+*	-	-	-	-	-	-	-	-	-	110.3	110.5
48	Palmatolepis gigas	311	532	+	O	O	-	-	-	O	*	O	O	122.0	133.1
49	Palmatolepis hassi sl	176	462	O	*	-	-	-	+	-	-	-	-	104.5	123.0
50	Palmatolepis hassi ss	312	429	+	*	-	-	-	-	-	-	-	-	122.3	127.5
51	Palmatolepis jamieae	272	489	+	*	-	-	-	-	-	-	-	-	109.3	125.7
52	Palmatolepis kireevae	293	312	+*	-	-	-	-	-	-	-	-	-	106.2	122.3
53	Palmatolepis linguiformis	529	530	-	+*	-	-	-	-	-	-	-	-	131.1	131.1
54	Palmatolepis ljashenkoae	293	312	+*	-	-	-	-	-	-	-	-	-	109.3	120.2
55	Palmatolepis muelleri	529	529	+	*	-	-	-	-	-	-	-	-	131.1	131.1
56	Palmatolepis nasuta	289	530	+	*	-	-	-	-	-	-	-	-	110.3	131.1
57	Palmatolepis paragigas	312	530	+	*	-	-	-	-	-	-	-	-	122.3	131.6
58	Palmatolepis perlobata perlobata	532	532	-	+*	-	-	-	-	-	-	-	-	132.1	132.1
59	Palmatolepis plana	176	334	+*	-	-	-	-	-	O	-	-	-	104.5	112.5
60	Palmatolepis praetriangularis	530	532	-	-	-	-	-	-	-	+*	-	-	131.2	131.4
61	Palmatolepis proversa	186	309	+*	O	-	-	-	O	-	-	-	-	104.7	111.7
62	Palmatolepis punctata	07 1	334	+*	-	-	-	-	-	O	-	-	-	100.8	112.5
63	Palmatolepis quadrantinodosalobata	534	534	-	-	-	-	-	-	-	+*	-	-	132.8	153.5
64	Palmatolepis rhenana	478	528	-	*	-	-	-	-	-	-	+	-	124.3	131
65	Palmatolepis rotunda	329	529	+	*	-	-	-	-	O	O	O	-	112.1	131.1
66	Palmatolepis semichatovae	306	312	+*	-	-	-	-	-	-	-	-	-	110.1	122.2
67	Palmatolepis simpla	247	332	+*	-	-	-	-	-	-	-	-	-	108.2	112.3
68	Palmatolepis spathula	532	532	-	+*	-	-	-	-	-	-	-	-	132.1	132.1
69	Palmatolepis subrecta	303	532	O	O	O	-	O	O	O	*	O	+	110.9	132.1
70	Palmatolepis timorensis	314	323	+*							O			111.4	111.9
71	Palmatolepis transitans	03 7	176	+*	-	-	-	-	-	O	-	-	-	99	104.5
72	Palmatolepis triangularis	532	532	-	O	-	-	-	-	O	*	+	O	131.4	141.0
73	Palmatolepis wildungensis	313	334	+*	O	-	-	-	-	-	-	-	-	111.4	112.4
74	Polygnathus aequalis	04 5	336	+*	-	-	-	-	-	-	-	-	-	100.7	112.6
75	Polygnathus alatus	0 01	336	+*	-	-	-	-	O	-	O	-	-	96.8	130.6
76	Polygnathus angustidiscus	0 02	333	*	-	-	-	-	-	-	+	-	-	96.5	124.6
77	Polygnathus brevis	335	335	+*	-	-	-	-	-	-	-	-	-	112.3	129.5
78	Polygnathus collieri	189	192	+*	-	-	-	-	-	-	-	-	-	96.6	105.1
79	Polygnathus decorosus	04 6	318	+*	-	-	-	O	-	-	-	-	-	100.7	131.3
80	Polygnathus denisbriceae	0 02	0 02	+*	-	-	-	-	-	-	-	-	-	97.7	97.7
81	Polygnathus dubius	000	189	+*	-	-	-	-	O	-	O	-	-	96.1	105
82	Polygnathus independensis	332	334	+*	-	-	-	-	-	-	-	-	-	112.3	112.5
83	Polygnathus pacificus	176	327	+*	-	-	-	-	-	-	-	-	-	103.5	131.3
84	Polygnathus webbi	0 02	448	+	-	*	-	-	O	-	-	O	-	96.9	131
85	Polygnathus xylus	000	199	+*	-	-	-	-	O	-	-	-	-	96.1	106.0

The fifth to 14th columns show the presence or absence of the taxa in the different sections.
+: First occurrence present
*: Last occurrence present
-: Species not found
O: Species found
The two last columns show the first and last occurrences of the Ardennes data that have been projected onto the KLAPPER composite. A greyish background indicates the conodont ranges that have been added to the Frasnian composite or the ranges that have been extended. The scale is given in Frasnian standard time units.

1978 *Ancyrodella rotundiloba* (BRYANT) - COEN, fig. 3, unit a (partim).
1982 *Ancyrodella rugosa* BRANSON & MEHL - BULTYNCK & JACOBS, tab. 1-2, pl. 2, figs. 11a, b, 13a, b- 16.
1985 *Ancyrodella rugosa* BRANSON & MEHL - KLAPPER, pl. 11, figs. 1, 2, 5-14, text-fig. 3U, V.
1989 *Ancyrodella rugosa* BRANSON & MEHL - VANDELAER, VANDORMAEL & BULTYNCK, pl. 1, figs. 3a, b, 4a, b.

Ancyrodella soluta SANDBERG, ZIEGLER & BULTYNCK, 1989

1989 *Ancyrodella soluta* n. sp. - SANDBERG, ZIEGLER & BULTYNCK, pl. 1, figs. 5-6, 11-12, pl. 2, figs. 1-4, text-fig. 2, figs. 5-7.

Genus *Ancyrognathus* BRANSON & MEHL, 1934
Ancyrognathus ancyrognathoideus (ZIEGLER, 1958) / ***Ancyrognathus primus*** JI, 1986

1958 *Polygnathus ancyrognathoidea* n. sp. - ZIEGLER, pp. 69-70, pl. 9, figs. 8, 16, 17, 20.
1974 *Polygnathus ancyrognathoideus* (ZIEGLER) - COEN, pl. 2, pl. 1.
1986 *Ancyrognathus primus* n. sp. - JI, pp. 28-29, 113, pl. 6, figs. 9-14.
1989 *Ancyrognathus ancyrognathoideus* (ZIEGLER) - VANDELAER, VANDORMAEL & BULTYNCK, pl. 3, fig. 6.
1990 *Ancyrognathus ancyrognathoideus* (ZIEGLER) - KLAPPER, figs. 2.10, 2.11, 3.8, 3.9.
1990 *Ancyrognathus primus* JI - KLAPPER, p. 1015, figs. 2.12-2.14
1992 *Ancyrognathus primus* JI - SANDBERG, ZIEGLER, DREESEN & BUTLER, pl. 8, figs. 5-6.
1992 *Ancyrognathus ancyrognathoideus* (ZIEGLER) - SANDBERG, ZIEGLER, DREESEN & BUTLER, pl. 8, figs. 1-4.

Ancyrognathus asymmetricus (ULRICH & BASSLER, 1926)

1926 *Palmatolepis asymmetrica* n. sp. - ULRICH & BASSLER, p. 50, pl. 7, fig. 18.
1970 *Ancyrognathus asymmetricus* (ULRICH & BASSLER) - COEN-AUBERT, pp. 391-392.
1974 *Ancyrognathus asymmetricus* (ULRICH & BASSLER) - COEN, pl. 1, pl. 4, pp. 81, 98, 100.
1974 *Ancyrognathus asymmetricus* (ULRICH & BASSLER) - COEN-AUBERT & COEN, p. 521.
1974 *Ancyrognathus asymmetricus* (ULRICH & BASSLER) - COEN-AUBERT, pp. 61, 67, 72.
1976 *Ancyrognathus asymmetricus* (ULRICH & BASSLER) - COEN & COEN-AUBERT, pp. 3, 4, 6.
1992 *Ancyroides asymmetricus* (ULRICH & BASSLER) - SANDBERG, ZIEGLER, DREESEN & BUTLER, pl. 6, figs. 7-9.
1998 *Ancyrognathus asymmetricus* (ULRICH & BASSLER) - BULTYNCK, HELSEN & HAYDUKIEWICZ, pl. 7, figs. 1-5.

Ancyrognathus coeni KLAPPER, 1990

1973 *Ancyrognathus triangularis euglypheus* STAUFFER - COEN, pp. 245, 247, text-fig. 2, fig. 24, text-fig. 3, figs. 2, 3, pl. 1, figs. 1, 2.
1974 *Ancyrognathus triangularis euglypheus* STAUFFER - COEN-AUBERT & COEN, pp. 517, 521.
1974 *Ancyrognathus triangularis euglypheus* STAUFFER - COEN, pl. 1-2, pl. 3, pp. 78, 81, 82, 86, 93, 96, 98.
1976 *Ancyrognathus triangularis euglypheus* STAUFFER - COEN & COEN-AUBERT, p. 2.
1990 *Ancyrognathus coeni* n. sp. - KLAPPER, figs. 5.1-5.4, 8.1, 8.4, 8.7, 8.8, 8.10, 8.11, 8.14, 9.1-9.16.

Ancyrognathus sinelobus (SANDBERG, ZIEGLER & DREESEN, 1992)

1992 *Ancyroides sinelobus* n. sp. SANDBERG, ZIEGLER & DREESEN *in* SANDBERG, ZIEGLER, DREESEN & BUTLER, pp. 57-58,pl. 10, figs. 7-8.
1998 *Ancyrognathus sinelobus* (SANDBERG, ZIEGLER & DREESEN) - BULTYNCK, HELSEN & HAYDUKIEWICZ, pl. 6, fig. 5.

Ancyrognathus triangularis YOUNGQUIST, 1945
Pl. 2 Figs. 7-8.

1945 *Ancyrognathus triangularis* n. sp. - YOUNGQUIST, pp. 356-357, pl. 54, fig. 7.
1970 *Ancyrognathus triangularis* YOUNGQUIST - COEN-AUBERT, pp. 390, 392.
1974 *Ancyrognathus triangularis triangularis* YOUNGQUIST - COEN, p. 247, text-fig. 3, figs. 9-13, pl. 1, figs. 3-5.
1974 *Ancyrognathus triangularis triangularis* YOUNGQUIST - COEN-AUBERT & COEN, pp. 517, 519, 520.
1974 *Ancyrognathus triangularis triangularis* YOUNGQUIST - COEN, pp. 69, 70, 72, 74, 77, 78, 81, 86, 88, 93, 98, 100, pl. 1-4.
1974 *Ancyrognathus triangularis* YOUNGQUIST - COEN-AUBERT, pp. 61, 67, 71.
1976 *Ancyrognathus triangularis triangularis* YOUNGQUIST - COEN & COEN-AUBERT, pp. 3, 4.
1978 *Ancyrognathus triangularis* YOUNGQUIST - COEN-AUBERT & LACROIX, pp. 270, 276.
1992 *Ancyrognathus triangularis* YOUNGQUIST - SANDBERG, ZIEGLER, DREESEN & BUTLER, p. 53, pl. 5, figs. 1-2, pl. 7, figs. 8-9, pl. 8, figs. 7-9.
1998 *Ancyrognathus triangularis* YOUNGQUIST - BULTYNCK, HELSEN & HAYDUKIEWICZ, tab. 1, 2, 3, 4a, b, 5, p. 56, pl. 6, figs. 6-7.

Ancyrognathus tsiensi MOURAVIEFF, 1982

1974 *Ancyrognathus triangularis euglypheus* STAUFFER - COEN, pl. 4, partim.
1982 *Ancyrognathus tsiensi* n.sp. - MOURAVIEFF, pp. 104-106, pl. 4, fig. 7, pl. 5, figs. 2-7, 11.
1989 *Ancyrognathus tsiensi* MOURAVIEFF - VANDELAER, VANDORMAEL & BULTYNCK, p. 3, fig. 7.

1992 *Ancyroides leonis* n. sp. - SANDBERG, ZIEGLER, DREESEN & BUTLER, pp. 56-57, pl. 4, figs. 4-10, pl. 5, figs. 3-6, pl. 6,fig. 1.
1992 *Ancyroides tsiensi* (MOURAVIEFF) - SANDBERG, ZIEGLER, DREESEN & BUTLER, p. 58, pl. 6, figs. 2-3.
1998 *Ancyrognathus tsiensi* MOURAVIEFF - BULTYNCK, HELSEN & HAYDUKIEWICZ, p. 56, pl. 6, fig. 11.

Genus *Klapperina* LANE, MÜLLER & ZIEGLER, 1979
Klapperina ovalis (ZIEGLER & KLAPPER, 1964)

1964 *Polygnathus asymmetricus ovalis* n. subsp. - ZIEGLER & KLAPPER, ZIEGLER *et al.*, pp. 422-423.
1982 *Polygnathus asymmetricus ovalis* ZIEGLER & KLAPPER - BULTYNCK & JACOBS, tab. 1-2, pl. 3, figs. 7, 17.
1989 *Mesotaxis ovalis* (ZIEGLER & KLAPPER) - KLAPPER, pl. 3, figs. 15-16.
1989 *Polygnathus asymmetricus ovalis* ZIEGLER & KLAPPER - VANDELAER, VANDORMAEL & BULTYNCK, tab. 2, 3, 5, 8, 9.
1990 *Klapperina ovalis* (ZIEGLER & KLAPPER) - ZIEGLER & SANDBERG, p. 43.

Klapperina unilabius (HUDDLE, 1981)
Pl. 1, Figs. 15-16.

1974 *Polygnathus asymmetricus* BISCHOFF & ZIEGLER - COEN, pl. 4, unit b'.
1981 *Polygnathus asymmetricus unilabius* n. sp. - HUDDLE, p. B26, pl. 7, figs. 13-15, pl. 8, figs. 4, 8-9, 11-12.
1986 *Polygnathus unilabius* HUDDLE - BULTYNCK, pl. 6, figs. 7, 10-12.
1989 *Polygnathus asymmetricus unilabius* HUDDLE - VANDELAER, VANDORMAEL & BULTYNCK, tab. 5, 8, 9.

Genus *Mesotaxis* KLAPPER & PHILIP, 1972
Mesotaxis asymmetricus (BISCHOFF & ZIEGLER, 1957)

1957 *Polygnathus dubia asymmetrica* n. subsp. - BISCHOFF & ZIEGLER, pp. 88-89, pl. 16, figs. 18, 20,
1974 *Polygnathus asymmetricus* BISCHOFF & ZIEGLER - COEN-AUBERT & COEN, p. 511.
1974 *Polygnathus asymmetricus* BISCHOFF & ZIEGLER - COEN, pp. 69, 84, 99, pl. 1, 2, 4.
1989 *Polygnathus asymmetricus asymmetricus* BISCHOFF & ZIEGLER - VANDELAER, VANDORMAEL & BULTYNCK, tab.2,4,5, 6, 8, 9.

Mesotaxis falsiovalis SANDBERG, ZIEGLER & BULTYNCK, 1989

1974 *Polygnathus asymmetricus* BISCHOFF & ZIEGLER - COEN, pl. 4, unit b.
1982 *Polygnathus asymmetricus* n. subsp. - ZIEGLER & KLAPPER, pl. 1, figs. 6a, 6b (reillustration of ZIEGLER, 1958, pl. 1, figs. 3a, 3b).
1989 *Mesotaxis falsiovalis* n. sp. - SANDBERG, ZIEGLER & BULTYNCK, p. 213.

Genus *Palmatolepis* ULRICH & BASSLER, 1926
Palmatolepis domanicensis OVNATANOVA, 1976
Pl. 2, Figs. 18-19.

1976 *Palmatolepis domanicensis* n. sp. - OVNATANOVA, p. 109, pl. 9, figs. 1,2.

Palmatolepis ljaschenkoae OVNATANOVA, 1976
Pl. 2, Figs. 20-21.

1976 *Palmatolepis ljaschenkoae* n. sp. - OVNATANOVA, p. 111-112, pl. 9, fig. 6.

Palmatolepis nasuta MÜLLER, 1956

1956 *Palmatolepis (Manticolepis) nasuta* n. sp. - MÜLLER, pp 23-24, pl. 6, figs. 31-33(only).
1990 *Palmatolepis rhenana nasuta* MÜLLER - ZIEGLER & SANDBERG, p. 57,pl. 12, figs. 4-9; pl. 15, fig. 4 (only).
1992 *Palmatolepis rhenana nasuta* MÜLLER - SANDBERG, ZIEGLER, DREESEN & BUTLER, pl. 2, fig. 7.
1992 *Palmatolepis rhenana rhenana* BISCHOFF - SANDBERG, ZIEGLER, DREESEN & BUTLER, pl. 2, fig. 6.
1992 *Palmatolepis rhenana nasuta* MÜLLER - HELSEN & BULTYNCK, pl. 3, fig. 13.
1998 *Palmatolepis nasuta* MÜLLER - BULTYNCK, HELSEN & HAYDUKIEWICZ, p. 59, pl. 5, figs. 3, 5-7.

Palmatolepis rotunda ZIEGLER & SANDBERG, 1990
Pl. 2, Figs. 10-12.

1974 *Palmatolepis subrecta* MILLER & YOUNGQUIST - COEN, pl. 1, unit m,k, pl. 4, unit j.
1988 *Palmatolepis bogartensis* (STAUFFER) - KLAPPER, p. 458, pl. 2, figs. 7-8.
1990 *Palmatolepis rotunda* n. sp. - ZIEGLER & SANDBERG, p. 62, pl. 10, figs. 1-5.
1993 *Palmatolepis bogartensis* (STAUFFER) - KLAPPER & FOSTER, pp. 17-18, figs. 13.4-13.16.
1998 *Palmatolepis rotunda* ZIEGLER & SANDBERG - BULTYNCK, HELSEN & HAYDUKIEWICZ, p. 60 pl. 4, figs. 1-11.

Palmatolepis subrecta MILLER & YOUNGQUIST, 1947
Pl. 2, Figs. 13-14.

1947 *Palmatolepis subrecta* n. sp. - MILLER & YOUNGQUIST, p. 513, pl. 75, figs. 7-11.
1974 *Palmatolepis subrecta* MILLER & YOUNGQUIST - COEN, pl. 1, 2, 4, pp. 72, 74, 77, 100.
1976 *Palmatolepis subrecta* MILLER & YOUNGQUIST - COEN & COEN-AUBERT, pp. 3-6.
1978 *Palmatolepis subrecta* MILLER & YOUNGQUIST - COEN-AUBERT & LACROIX, p. 270.
1985 *Palmatolepis subrecta* MILLER & YOUNGQUIST - COEN-AUBERT & LACROIX,p. 121.
non 1992 *Palmatolepis subrecta* MILLER & YOUNGQUIST - SANDBERG, ZIEGLER, DREESEN & BUTLER, pl. 2, figs. 4, 5.
1993 *Palmatolepis winchelli* (STAUFFER) - KLAPPER & FOSTER, pp. 24-31, figs. 13.1, 13.2, figs. 18.3-18.7.

1998 *Palmatolepis subrecta* MILLER & YOUNGQUIST - BULTYNCK, HELSEN & HAYDUKIEWICZ, p. 60, pl. 3, figs. 8-13.

Palmatolepis timanensis KLAPPER, KUZ'MIN & OVNATANOVA, 1996
Pl. 2, Fig. 9.

1996 *Palmatolepis timanensis* n. sp. - KLAPPER, KUZ'MIN & OVNATANOVA, p. 149, figs. 9.1-9.4.

Remark: Palmatolepis timanensis was found in an additional sample between unit i' and unit j in COEN (1974: pl. 1, Verlaine)

Conclusions

1. The Ardennes Frasnian Regional Composite developed in this study integrates ranges of 85 conodont taxa, 48 coral taxa, 29 brachiopod taxa and one stromatoporoid taxon. This chronostratigraphic framework provides the best possible stratigraphic resolution for the Frasnian of the Ardennes region. It allows a subdivision of the Frasnian into 532 composite standard units, derived from the standard reference section in the southern part of the Dinant Synclinorium, because the uppermost part of the Frasnian is not exposed in this area the SRS has been completed with a section in the Philippeville Massif. It also allows a more precise determination of the magnitude of diachronism (see Table 2) for the four distinguished diachronous deposits.

The first bioherm development phase in the southern part of the Dinant Synclinorium corresponds to the first biostrome development phase in the southeastern and northern part of the Dinant Synclinorium and in the Namur Synclinorium. The second bioherm development phase in the southern part of the Dinant Syclinorium is correlated with the second biostrome development phase in the southeastern and northern part of the Dinant Synclinorium and in the Namur Synclinorium.

Correlation between the regional composite of the Ardennes and the Frasnian CS (KLAPPER 1997) can add new data to the latter and can extend a few ranges of taxa, already incorporated in the Frasnian CS. The correlation also indicates that the first occurrence of some taxa in the Ardennes is delayed compared to the Frasnian CS (Fig. 19) (*Ancyrodella curvata* (early), *Ad. curvata* (late), *Polygnathus collieri, Palmatolepis transitans, Pal. kireevae, Pal. ederi, Pal. semichatovae, Ancyrognathus triangularis, Ancyrodella nodosa* and *Palmatolepis domanicensis*). Therefore these taxa cannot be directly used for precise long-distance correlations.

2. Based on the diachronous nature of the deposits and the conodont biofacies analysis, we can distinguish four major T-R cycles. The first one corresponds with the IIb cycle of JOHNSON *et al.* (1985) and contains the development of the first diachronous limestone bar. The second and the third major T-R cycles (cycle IIc) encompassing the *punctata* Zone respectively the *hassi* sl Zone corre-

Table 2 — Magnitude of diachronism in the Frasnian of the Ardennes.

	Locality	Present distance	Estimated original distance	Magnitude of diachronism
Base Nismes Fm.	Nismes – Tailfer	44 km	>120 km	1.5 m
	Nismes – Sy	80 km	± 110 km	1.5 m
Base Chalon Mbr. /Font. Samart Mbr. /base Lustin Fm.	Nismes – Tailfer	44 km	>120 km	6.5 m
	Nismes – Sy	80 km	± 110 km	10 m
Base Bieumont Mbr./ base Philippeville Fm. in MPH/ base second biostrome of Lustin Fm.	Nismes – Senzeilles	10 km	±30 km	20 m
	Nismes	44 km	± 110 km	15 m
Base Neuville Fm. /Aisemont Fm.	Senzeilles – Tailfer	36 km	>105 km	6 m
	Sy – Remouchamps	17 km	± 20 km	3 m

spond with the first two bioherm development phases. The fourth T-R cycle (cycle IId) starting in the Early *rhenana* Zone and continuing till the upper part of the Late *rhenana* Zone corresponds to the interval with development of the red mudmounds. The first, second and fourth T-R-cycles are also recognised in the New York area and in Western Canada and can thus be considered as eustatic. Taking into account the duration of the conodont zones, we consider the major T-R-cycles as cycles of third order (500.000y- 5 m.y.) and the minor T-R-cycles as cycles of fourth order (100.000y-500.000y). The Lower Kellwasser Event could agree well with the transgression in the lower part of the Late *rhenana* Zone at the base of the Matagne Formation in the Southern part of the Dinant Synclinorium. The Upper Kellwasser Event was recognised in the Matagne shales equivalent of the eastern part of the Dinant Synclinorium (*linguiformis* Zone) (SANDBERG *et al.*, 1988) and at the base of the Matagne Formation in the Philippeville Massif (BULTYNCK *et al.*, 1998).

Acknowledgements

The authors acknowledge M. COEN (Louvain-la-Neuve) for allowing us to study his conodont collections from Barvaux, Aisne, Verlaine, Sy, Tohogne, Sinsin, Comblain-la-Tour, Aywaille, Remouchamps, Louveigne, Durbuy and Bohon. We also thank Z. BELKA (Eberhard-Karls Universität Tübingen, Germany) for introducing us to the Graphic Correlation Method and Kenneth C. HOOD (Houston) for providing us with the *Graphcor* program for PC.

M. COEN, Z. BELKA and E. STEURBAUT (KBIN, Brussels) also reviewed an earlier version of the manuscript and made many valuable comments.

References

AUBERT, M., 1968. Observations sur le Frasnien de Pepinster et Trooz. *Annales de la Société Géologique de Belgique*, **91** (3): 347-360.

BISCHOFF, G. & ZIEGLER, W., 1957. Die Conodontenchronologie des Mitteldevons und des tiefsten Oberdevons. *Abhandlungen des Hessischen Landesamtes für Bodenforschung*, **22**: 1-136.

BLOOM, A. L., 1974. Geomorphology of reef complexes, *In*: LAPORTE, L., F. (Ed.) Reefs in time and Space. *Society of Economic Paleontologists and Mineralogists, Special Publication*, **18**: 1-9.

BOUHARRAK, M., 1984. Lithostratigrafie en biostratigrafie (conodonten) en struktuur van het Boven Givetiaan en het Frasniaan in het gebied van Ave-et-Auffe. Unpublished thesis K.U.Leuven, 102 pp.

BOULVAIN, F., BULTYNCK, P., COEN, M., COEN-AUBERT, M., LACROIX, D., LALOUX, M., CASIER, J.-G., DEJONGHE, L., DUMOULIN, V., GHYSEL, P., GODEFROID, J., HELSEN, S., MOURAVIEFF, N.A., SARTENAER, P., TOURNEUR, F. & VANGUESTAINE, M., 1999. Les Formations du Frasnien de la Belgique. *Memoirs of the Geological Survey of Belgium*, **44**: 1-126.

BOULVAIN, F., COEN-AUBERT, M., DUMOULIN, V. & MARION, J-M., 1994. La Formation de Philippeville à Merlemont: contexte structural, comparaison avec le stratotype et paleoenvironnements. *Service Géologique de Belgique, Professional Paper*, **269**: 29pp.

BRANSON, E. B. & MEHL, M. G., 1934. Conodonts of the Grassy Creek shale of Missouri. *The University of Missouri Studies*, **8**: 171-259.

BRYANT, W. L, 1921. The Genesee Conodonts with descriptions of New Species. *Bulletin of the Buffalo Society of Natural Sciences*, **13**: 1-59.

BULTYNCK, P., 1974. Conodontes de la Formation de Fromelennes du Givetien de l'Ardenne franco-belge. *Bulletin de l'Institut royal des Sciences naturelles de Belgique, Sciences de la Terre*, **50** (10): 30pp.

BULTYNCK, P., 1986. Accuracy and reliability of conodont zones: the *Polygnathus asymmetricus* 'zone' and the Givetian-Frasnian boundary. *Bulletin de l'Institut royal des Sciences naturelles de Belgique, Sciences de la Terre*, **56**: 269-280.

BULTYNCK., P., CASIER., J. G., COEN., M., COEN.-AUBERT., M., GODEFROID., J., JACOBS., L., LOBOZIAK., S., SARTENAER., P. & STREEL., M., 1988a. Pre -Congres excursion to the Devonian stratotypes in Belgium. *Bulletin de la Société belge de Géologie*, **96**: 249-288.

BULTYNCK., P., HELSEN., S. & HAYDUKIEWICZ., J, 1998. Conodont succession and biofacies in upper Frasnian formations (Devonian) from the southern and central parts of the Dinant Synclinorium (Belgium) - (Timing of facies shifting and correlation with late Frasnian events). *Bulletin de l'Institut royal des Sciences naturelles de Belgique, Sciences de la Terre*, **68**: 25-75.

BULTYNCK, P. with contribution by JACOBS, L., 1982. Conodont succession and general faunal distribution across the Givetian-Frasnian boundary beds in the type area. *In*: Papers on the Frasnian-Givetian boundary, Geological Survey of Belgium, Brussels, pp. 34-59.

COEN, M., 1973. Faciès, conodontes et stratigraphie du Frasnien de l'est de la Belgique, pour servir à une révision de l'étage. *Annales de la Société Géologique de Belgique*, **95** (2): 239-253.

COEN, M., 1974. Le Frasnien de la bordure orientale du Bassin de Dinant. *Annales de la Société Géologique de Belgique*, **97** (1): 67-103.

COEN, M., 1977. La Klippe du Bois Niau. *Bulletin de la Société belge de Géologie*, **86**: 41-44.

COEN, M., 1978. Le Givetien et le Frasnien dans le contournement routier de Philippeville. Comparaison avec la coupe de Neuville. *Annales de la Société Géologique de Belgique*, **100**: 23-30.

COEN, M. & COEN-AUBERT, M., 1971. L'assise de Fromelennes aux bords sud et est du bassin de Dinant et dans le massif de la Vesdre. *Annales de la Société Géologique de Belgique*, **94** (1): 5-20.

COEN, M. & COEN-AUBERT, M., 1976. Conodontes et Coraux de la partie supérieure du Frasnien dans la tranchée du chemin de fer de Neuville (Massif de Philippeville, Belgique). *Bulletin de l'Institut royal des Sciences naturelles de Belgique, Sciences de la Terre*, **50** (8): 1-7.

COEN, M., COEN-AUBERT, M. & CORNET, P., 1976. Distribution et extension stratigraphique des récifs à *"Phillipsastrea"* dans

le Frasnien de l'Ardenne. *Annales de la Société Géologique de Belgique*, **96** (4): 325-331.

COEN-AUBERT, M., 1969. Le Givetien et le Frasnien inférieur de Pepinster. *Annales de la Société Géologique de Belgique*, **92** (3): 383-395.

COEN-AUBERT, M., 1970. Le Frasnien dans la région des Surdents (Massif de la Vesdre, Belgique). *Annales de la Société Géologique de Belgique*, **93** (2): 383-394.

COEN-AUBERT, M., 1974. Le Givetien et le Frasnien du massif de la Vesdre. Stratigraphie et paléogéographie. *Mémoires de la Classe des Sciences de l'Académie royale de Belgique*, Collection in 4E, 2^{e} série, **18** (2): 1-146.

COEN-AUBERT, M., 1980a. Représentants frasnien du genre *Scruttonia* Tcherepnina, S. K., 1974 (Rugosa) en Belgique. *Bulletin de l'Institut royal des Sciences naturelles de Belgique, Sciences de la Terre*, **51** (4):1-15.

COEN-AUBERT, M., 1980b. Rugueux massifs ceroïdes du Givetien et du Frasnien de la Belgique. *Bulletin de l'Institut royal des Sciences naturelles de Belgique, Sciences de la Terre*, **51** (14): 1-53.

COEN-AUBERT, M., 1982. Rugueux solitaires du Frasnien de la Belgique. *Bulletin de l'Institut royal des Sciences naturelles de Belgique, Sciences de la terre*, **54**(6): 1-65.

COEN-AUBERT, M., 1986a. Nouvelles sous-espèces de *Phillipsastrea hennahi* (LONSDALE, W., 1840) dans le Frasnien supérieur de la Belgique. *Bulletin de l'Institut royal des Sciences naturelles de Belgique, Sciences de la Terre*, **56**: 45-55.

COEN-AUBERT, M., 1986b. Description de deux espèces de *Wapitiphyllum* MCLEAN, R.A. et PEDDER, A.E.H., 1984 récoltées dans le Frasnien de Huccorgne, au bord nord du Bassin de Namur. *Bulletin de l'Institut royal des Sciences naturelles de Belgique, Sciences de la Terre*, **56**: 57-65.

COEN-AUBERT, M., 1994. Stratigraphie et systématique des Rugueux de la partie moyenne du Frasnien de Frasnes-lez-Couvin (Belgique). *Bulletin de l'Institut royal des Sciences naturelles de Belgique, Sciences de la Terre*, **64**: 21-56.

COEN-AUBERT, M., 1999. Extension Stratigraphique des rugueux dans le Frasnien. *In*: BOULVAIN *et al.*, Les Formations du Frasnien de la Belgique. *Memoirs of the Geological Survey of Belgium*, **44**: 16-18.

COEN-AUBERT, M. & COEN, M., 1974. Le Givetien et le Frasnien dans la vallée de la Meuse de Tailfer à Yvoir (bord nord du Bassin de Dinant). *Annales de la Société Géologique de Belgique*, **97** (2): 499-524.

COEN-AUBERT, M. & LACROIX, D., 1979. Le Frasnien dans la partie orientale du bord sud du synclinorium de Namur. *Annales de la Société Géologique de Belgique*, **101**: 269-279.

COEN-AUBERT, M. & LACROIX., D, 1985. Le Frasnien dans la partie orientale du bord nord du Synclinorium de Namur. *Bulletin de la Société belge de Géologie*, **94**: 117-128.

DUMOULIN, V., BERTRAND, M. & PREAT, A., 1996. Microfacies et cyclicité au sein d'un complexe biostromal de la partie moyenne du Frasnien à Cerfontaine "Massif de Philippeville" synclinorium de Dinant (Belgique). *Bulletin de la Société belge de Géologie*, **105** (3-4): 99-118.

EINSELE, G., RICKEN, W. & SEILACHER, A. (Eds.), 1991. Cycles and Events in Stratigraphy. Springer-Verlag, Berlin, 955pp.

EMERY, D. & MYERS, K., J. (Eds.) with contributions from BERTRAM, G., GRIFFITHS, C., MILTON, N., REYNOLDS, T., RICHARDS, M. & STURROCK, S., 1996. Sequence stratigraphy. Blackwell Science Ltd, Oxford, 297pp.

GARCÍA-LÓPEZ, S., 1981. Nueva especie de *Ancyrodella* (Conodonta) del Devónico superior de la Cordillera Cantábrica (NO de España). *Estudios Geológicos*, **37**:263-267.

GLENISTER, B. F. & KLAPPER, G., 1966. Upper Devonian conodonts from the Canning basin, Western Australia. *Journal of Paleontology*, **40**: 777-842.

GODEFROID, J., 1994. *Iowatrypa rotundicollis* n. sp. , brachiopode atrypé de la fin du Frasnien. *Bulletin de l'Institut royal des Sciences naturelles de Belgique, Sciences de la Terre*, **64**: 85-95.

GODEFROID, J., 1998. Le genre *Costatrypa* COPPER, 1973 (Brachiopoda, Atrypa) dans le Frasnien du sud de la Belgique. *Bulletin de l'Institut royal des Sciences naturelles de Belgique, Sciences de la Terre*, **68**: 97-114.

GODEFROID, J., 1999. Répartition Stratigraphique des principaux brachiopodes gypidulinés et atrypidés dans le Frasnien. *In* BOULVAIN *et al.*, Les Formations du Frasnien de la Belgique. *Memoirs of the Geological Survey of Belgium*, **44**: 19-20.

GODEFROID, J. & HELSEN, S., 1998. The last Frasnian Atrypida (Brachiopoda) in southern Belgium. *Acta Palaeontologica Polonica*, **43** (2): pp. 241-272.

GODEFROID, J. & JACOBS, L., 1986. Atrypidae (Brachiopoda) de la Formation de Fromelennes (fin du Givetien) et de la partie inférieure de la Formation de Nismes (début du Frasnien) aux bords sud et sud-est du Synclinorium de Dinant (Belgique). *Bulletin de l'Institut royal des Sciences naturelles de Belgique, Sciences de la Terre*, **56**: 67-136.

HELSEN, S. & BULTYNCK, P., 1992. Conodonts and megafauna from two sections at Nismes and Mariembourg (Frasnian of the southern flank of the Dinant synclinorium, Belgium). *Annales de la Société géologique de Belgique*, **115** (1): 145-157.

HOOD, K. C., 1998. Graphcor, Interactive Graphic Correlation software. Houston, Hood, Kenneth C.

HUDDLE, J. W., assisted by REPETSKI, J., 1981. Conodonts from the Genesee Formation in western New York. *U.S. Geological Survey Professional Paper*, **1032-B**: 1-66.

JI, Q., 1986. Research on the Middle/Upper Devonian boundary at Dale, Guangxi. *Acta Micropalaeontologica Sinica*,

3: 89-98.

JOHNSON, J. G., KLAPPER G. & SANDBERG C. A., 1985. Devonian eustatic fluctuations in Euramerica. *Geological Society of America Bulletin*, **96**: 567-587.

KHALYMBADZHA, V. G. & CHERNYSHEVA N. G., 1970. Conodont genus *Ancyrodella* from Devonian deposits of the Volga-Kamsky area and their stratigraphic significance. *In*: Biostratigraphy and paleontology of Paleozoic deposits of the eastern Russian Platform and western pre-Urals (in Russian). Kazan University, **1**: 81-103.

KLAPPER, G., 1985. Sequence in conodont genus *Ancyrodella* in Lower *asymmetricus* Zone (earliest Frasnian, Upper Devonian) of the Montagne Noire, France. *Palaeontographica A*, **188**: 19-34.

KLAPPER, G., 1988. The Montagne Noire Frasnian (Upper Devonian) conodont succession. *In*, Mc Millan, N. J., Embry A. F.and Glass, D. J. (Eds.), Devonian of the World: Calgary. *Canadian Society of Petroleum Geologists Memoir*, **14:** 449-468.

KLAPPER, G., 1990. Frasnian species of the Late Devonian conodont genus *Ancyrognathus*. *Journal of Paleontology*, **64** (6): 998-1025.

KLAPPER, G., 1997. Graphic correlation of Frasnian (Upper Devonian) sequences in Montagne Noire, France, and Western Canada. *Geological Society of America Special Paper*, **321**: 113-129.

KLAPPER, G. & FOSTER, C. T. Jr., 1993. Shape analysis of Frasnian species of the Late Devonian conodont genus *Palmatolepis*. *The Paleontological Society Memoir*, **32**: 1-35.

KLAPPER, G., KUZ'MIN, A. V. & OVNATANOVA, N.S., 1996. Upper Devonian conodonts from the Timan-Pechora region, Russia and correlation with a Frasnian composite standard. *Journal of Paleontology*, **70** (1): 131-151.

KLAPPER, G. & PHILIP, G.M., 1972. Familial classification of reconstructed Devonian conodont apparatuses. *Geologica et Palaeontologica*, **SB1**: 97-114.

LACROIX, D., 1974. Sur la stratigraphie du Mésodévonien et du Frasnien au bord sud du Synclinorium de Namur. *Annales de la Société Géologique de Belgique*, **97** (1): 11-21.

LANE, H. R., MÜLLER, K. J. & ZIEGLER, W., 1979. Devonian and Carboniferous conodonts from the Perak Malaysia, *Geologica et Palaeontologica*, **13**: 213-226.

LECOMPTE, M., 1967. Le Devonien de la Belgique et le Nord de la France. International Symposium on the Devonian System, Calgary. *Alberta Society of Petroleum Geologists*, **1**: 15-52.

MILLER, A. K. & YOUNGQUIST, W., 1947. Conodonts from the type section of the Sweetland Creek Shale in Iowa. *Journal of Paleontology*, **21**: 501-517.

MOURAVIEFF, A. N., 1974. Excursion F. International Symposium on Belgian micropaleontological limits from Emsian to Visean, Namur 1974. Service Géologique de Belgique, Bruxelles, pp. 1-13.

MOURAVIEFF, A .N., 1982. Conodont stratigraphic scheme of the Frasnian of the Ardennes. *In*: Papers on the Frasnian-Givetian boundary. Geological Survey of Belgium, Brussels, pp. 101-118.

MÜLLER, K. J., 1956. Zur Kenntnis der Conodonten-Fauna des europäischen Devons, 1. Die Gattung *Palmatolepis*. *Abhandlungen der Senckenbergischen Naturforschenden Gesellschaft*, **494**: 1-70.

OVNATANOVA, N. S., 1976. Novye pozdnedevonskie konodonty Russkoy Platformy. *Paleontologicheskiy Zhurnal*, **2**: 106-115.

PHILLIPS, J. F., 1986. A Review of Graphic Correlation. *COGS Computer Contributions*, **2**(2): 73-91.

SANDBERG, C. A. & DREESEN, R., 1984. Late Devonian icriodontid biofacies models and alternate shallow-water conodont zonation. *Geological Society of America, Special Paper*, **196**:143-178.

SANDBERG, C. A. & ZIEGLER, W., 1979. Taxonomy and biofacies of important conodonts of Late Devonian *styriacus*-Zone, United States and Germany. *Geologica et Palaeontologica*, **13**:173-212.

SANDBERG, C. A. & ZIEGLER, W., 1996. Devonian conodont biochronology in geologic time calibration. *Senckenbergiana lethaea*, **76**: 259-265.

SANDBERG, C. A., ZIEGLER, W. & BULTYNCK, P., 1989. New Standard Conodont Zones and Early *Ancyrodella* Phylogeny across Middle-Upper Devonian Boundary. *Courier Forschungsinstitut Senckenberg*, **110**: 195-230.

SANDBERG, C. A., ZIEGLER, W., DREESEN, R. & BUTLER, J. L., 1988. Late Frasnian mass extinction: conodont event stratigraphy, global changes, and possible causes. *In*: Ziegler, W. (Ed.), 1st International Senckenberg Conference and 5th European Conodont Symposium 'ECOS V), *Contribution 1. Courier Forschungsinstitut Senckenberg*, **102**: 263-307.

SANDBERG, C. A., ZIEGLER, W., DREESEN, R. & BUTLER, J. L., 1992. Conodont biostratigraphy around Middle Frasnian Lion Mudmound (F2h), Frasnes, Belgium. *Courier Forschungsinstitut Senckenberg*, **150**: 1-87.

SARTENAER, P., 1999. Répartition Stratigraphique des principaux brachiopodes rhynchonellidés et spiriféridés dans le Frasnien. *In*: BOULVAIN *et al.*, Les Formations du Frasnien de la Belgique. *Memoirs of the Geological Survey of Belgium*, **44**: 21-23.

SEDDON, G. & SWEET, W. C., 1971. An ecologic model for conodonts. *Journal of Paleontology*, **45**: 869-880.

TSIEN, H. H., DRICOT, E., MOURAVIEFF, A.N. & BOUCKAERT, J., 1973. Le Frasnien de la coupe de Tailfer. *Service Géologique de Belgique, Professional Paper*, **11**: 1-13.

TUCKER, R. D., BRADLEY, D. C., VER STRAETEN, C. A., HARRIS, A. G., EBERT, J. R. & MCCUTCHEON, S. R., 1998. New U-Pb zircon ages and the duration and division of Devonian time. *Earth and Planetary Science Letters*, **158**: 175-186.

ULRICH, E. O. & BASSLER, R. S., 1926. A classification of the toothlike fossils, conodonts, with descriptions of American Devonian and Mississippian species. *Proceedings of the U. S. National Museum*, **68** (12): 1-63.

UYENO, T. T., 1967. Conodont zonation, Waterways Formation (Upper Devonian), northeastern and Central Alberta. *Geological Survey of Canada Paper*, **67-30**: 1-21.

VAIL, P.R., JACQUIN, T. & WOMART, W., 1991. High resolution sequence stratigraphy and biostratigraphy. *In*: LECKIE, D., POSAMENTIER, H. & LOWELL, R. (Eds.), NUNA Conference on high-resolution sequence stratigraphy. The Geological Association of Canada, Toronto, pp. 55-56

VANDELAER, E., VANDORMAEL, C. & BULTYNCK, P., 1989. Biofacies and refinement of Conodont Succession in the Lower Frasnian (Upper Devonian) of the Type Area (Frasnes-Nismes, Belgium). *Courier Forschungsinstitut Senckenberg*, **117**: 321-351.

YOUNGQUIST, W. L., 1945. Upper Devonian conodonts from the Independence Shale (?) of Iowa. *Journal of Paleontology*, **19**: 355-367.

YOUNGQUIST, W. L., 1947. A new Upper Devonian condont fauna from Iowa. *Journal of Paleontology*, **21**: 95-112.

ZIEGLER, W., 1958. Conodontenfeinstratigraphische Untersuchungen an der Grenze Mitteldevon/Oberdevon und in der Adorf-stufe. *Notizblatt des Hessischen Landesamtes für Bodenforschung*, **87**: 7-77.

ZIEGLER, W., KLAPPER, G. & LINDSTRÖM, M., 1964. The validity of the name *Polygnathus* (Conodonta, Devonian and Lower Carboniferous). *Journal of Paleontology*, **38**: 421-423.

ZIEGLER, W. & KLAPPER, G., 1982. The *disparilis* Conodont Zone, the proposed level for the Middle-Upper Devonian Boundary. *Courier Forschungsinstitut Senckenberg*, **55**: 463-492.

ZIEGLER, W. & SANDBERG, C. A., 1990. The Late Devonian standard conodont zonation. *Courier Forschungsinstitut Senckenberg*, **121**: 1-115.

Sofie GOUWY
Afd. Historische Geologie - Instituut voor Aardwetenschappen
Redingenstraat 16, B-3000 Leuven,
Belgium
(e-mail:sofie.gouwy@geo.luleuven.ac.be)

Pierre BULTYNCK
Dept. of Palaeontology
Koninklijk Belgisch Instituut voor Natuurwetenschappen
Vautierstraat 29, B-1000 Brussels,
Belgium
(e-mail: *bultynck@kbinirsnb.be*)

Typescript submitted: 1.12.1999
Revised typescript received: 20.4.2000

PLATE 1

All magnifications are x 59.

Figs. 1, 2 — *Ancyrodella rotundiloba* (BRYANT, 1921).
Sy, lowest part of the Nismes Formation.
Collection COEN 1974, pl. 1, unit a.
Upper and lower views. I.R.Sc.N.B. N°b 3671, N°b 3672

Figs. 3-6 — *Ancyrodella rugosa* BRANSON & MEHL, 1934.
Philippeville south, lowest part of the Nismes Formation.
Collection COEN 1978, fig. 3, unit a.
Upper and lower views. I.R.Sc.N.B. N°b 3673, N°b 3674.

Figs. 7, 8 — *Ancyrodella africana* GARCÍA-LÓPEZ, 1981.
Sy, lowest part of the Nismes Formation.
Collection COEN 1974, pl. 1, unit a.
Upper and lower views. I.R.Sc.N.B. N°b 3675.

Figs. 9, 10 — *Ancyrodella gigas* YOUNGQUIST, 1947.
Tohogne, Machenées Member.
Collection COEN 1974, pl. 1, unit b.
Upper and lower views. I.R.Sc.N.B. N°b 3676.

Figs. 11, 12 — *Ancyrodella gigas* YOUNGQUIST, 1947.
Barvaux south, middle part of the Chalon Member.
Collection COEN 1974, pl. 4, unit b.
Upper and lower views. I.R.Sc.N.B. N°b 3677.

Figs. 13, 14 — *Ancyrodella lobata* BRANSON, & MEHL, 1934.
Philippeville south, middle part of the Machenées Member.
Collection COEN 1978, fig. 3, unit e.
juvenile specimen, upper and lower views. I.R.Sc.N.B. N°b 3678.

Fig. 15, 16 — *Klapperina unilabius* (HUDDLE, 1981).
Barvaux south, lower part of the Ermitage Member.
Collection COEN 1974, pl. 4, unit b'.
Upper and lower views. I.R.Sc.N.B. N°b 3679.

PLATE 2

All magnifications are x 59.

Figs. 1, 2 — *Ancyrodella curvata* (BRANSON & MEHL, 1934) late form.
Barvaux, top of bioherm in the Valisettes Formation.
Collection COEN 1974, Jastrée, fig. 10.
Lower and upper views. I.R.Sc.N.B. N°b 3 680.

Fig. 3 — *Ancyrodella curvata* (BRANSON & MEHL, 1934) late form.
Verlaine, upper part of the Barvaux Formation, close to the Frasnian/Famennian boundary.
Collection COEN, 1974, pl. 1, unit m.
Upper view. I.R.Sc.N.B. N°b 3681.

Fig. 4 — *Ancyrodella curvata* (BRANSON & MEHL, 1934) latest form.
Barvaux, bioherm in the Valisettes Formation.
Collection COEN, 1974, Pl. 4, Jastrée, fig. 10.
Upper view. I.R.Sc.N.B. N°b 3682.

Figs. 5, 6 — *Ancyrodella curvata* (BRANSON & MEHL, 1934) early form.
Barvaux north, middle part of the Bieumont Member.
Collection COEN 1974, pl. 4, unit e.
Upper and lower views. I.R.Sc.N.B. N°b 3683.

Figs. 7, 8 — *Ancyrognathus triangularis* YOUNGQUIST, 1945.
Verlaine, upper part of the Neuville Formation.
Collection COEN 1974, pl. 1, fig. 4, section 8.
Upper and lower views. I.R.Sc.N.B. N°b 3684.

Fig. 9 — *Palmatolepis timanensis* KLAPPER, KUZ'MIN & OVNATANOVA, 1996.
Verlaine, upper part of the Neuville Formation.
Collection COEN 1974, pl. 1, fig. 4, section 8.
Upper view. I.R.Sc.N.B. N°b 3685.

Fig. 10 — *Palmatolepis rotunda* ZIEGLER, & SANDBERG, 1990.
Verlaine, upper part of the Barvaux Formation, close to the Frasnian/Famennian boundary.
Collection COEN 1974, pl. 1, unit m.
Upper view. I.R.Sc.N.B. N°b 3686.

Fig. 11 — *Palmatolepis rotunda* ZIEGLER, & SANDBERG, 1990.
Aywaille, lower part of the Lambermont Formation.
Collection COEN 1974, pl. 1, unit k.
Upper view. I.R.Sc.N.B. N°b 3687.

Fig. 12 — *Palmatolepis rotunda* ZIEGLER, & SANDBERG, 1990.
Barvaux south, lowest part of the Barvaux Formation.
Collection COEN 1974, pl. 4, unit i.
Upper view. I.R.Sc.N.B. N°b 3688.

Fig. 13 — *Palmatolepis subrecta* MILLER, & YOUNGQUIST, 1947.
Verlaine, upper part of the Barvaux Formation, close to the Frasnian/Famennian boundary.
Collection COEN 1974, pl. 1, unit m.
Upper view. I.R.Sc.N.B. N°b 3689.

Fig. 14 — *Palmatolepis subrecta* MILLER, & YOUNGQUIST, 1947.
Nismes, lowermost part of the Matagne Formation.
Collection BULTYNCK, HELSEN, & HAYDUCKIEWICH, 1998, sample C 16.
Upper view. I.R.Sc.N.B. N°b 3690.

Fig. 15 — *Palmatolepis cf. foliacea* YOUNGQUIST, 1945.
Nismes, lowermost part of the Matagne Formation.
Collection BULTYNCK, HELSEN, & HAYDUCKIEWICH, 1998, sample C 16.
Upper view. I.R.Sc.N.B. N°b 3691.

Fig. 16 — *Palmatolepis praetriangularis* ZIEGLER, & SANDBERG, 1988.
Barvaux, uppermost part of the Barvaux Formation.
Collection COEN 1974, pl. 4, unit k.
Upper view. The posterior carina declines downwards. I.R.Sc.N.B. N°b 3692.

Fig. 17 — *Palmatolepis triangularis* SANNEMANN, 1955.
Barvaux, lowermost part of the Senzeilles Formation.
Collection COEN 1974, pl. 4, unit k.

Upper view. The posterior carina rises abruptly posteriorward from the central node. I.R.Sc.N.B. N°b 3693.

Figs. 18-19 — *Palmatolepis domanicensis* OVNATANOVA, 1976.
Frasnes, railroad cut west of Carrière du Lion, upper part of the Boussu-en-Fagne Member.
Collection VANDELAER, unpublished, sample Fr 82, 95m above thick-bedded part of the Bieumont Member.
Upper views. I.R.Sc.N.B. N°b 3694, N°b 3695.

Figs. 20-21 — *Palmatolepis ljashenkoae* OVNATOVA, 1976.
Frasnes, railroad cut west of Carrière du Lion, upper part of the Boussu-en-Fagne Member.
Collection VANDELAER, unpublished, sample Fr 80, 93m above thick bedded part of the Bieumont Member.
Upper views. I.R.Sc.N.B. N°b 3696, N°b 3697.

PLATE 1

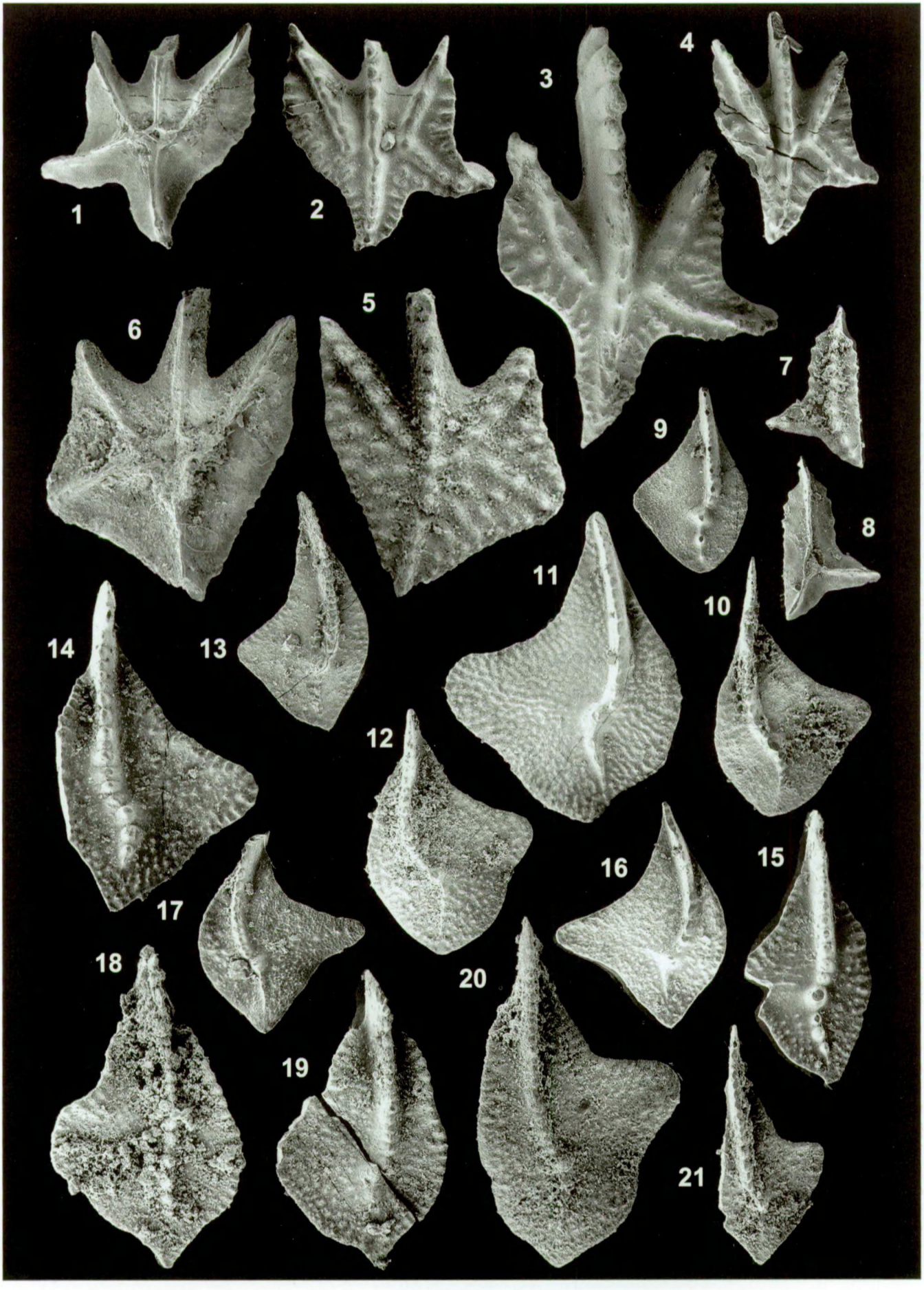

PLATE 2